

1 Replies and revised text in response to two reviewer comments are identical to those published online
2 in ACPD, with the exception of one update (highlighted in red).

3 4 **Reply to comments of Referee No.1**

5 We thank Referee No.1 for insightful comments which helped to further improve the manuscript. Ref-
6 eree comments (in italics) are addressed below. Revised text, where necessary, is shown in blue,
7 and is included in the final manuscript we will submit to ACP.

8
9 *General: I enjoyed the paper and appreciate the challenges in linking NO_x chemistry, the diurnal
10 cycle, and boundary layer effects. The discussion of limitations in the evaluation of the effects of
11 interferences was quite complete. It is clear that much has been accomplished but more remains
12 to be done. A peeve of mine that the various papers in this collection do not appear to have been
13 coordinated in the time Periods highlighted (particularly in the figures): For example, Gallée et al
14 provides details on model versus observed boundary layer depth for 26-28 December but the really
15 interesting chemistry is earlier in Periods II and III in Frey. Similarly earlier published work (Argentini
16 et al.) looked carefully at 10 January boundary layer behaviour but Frey et al. did detailed profile
17 measurements a day earlier. It would be useful in collections such as these to identify specific Periods
18 of common interest prior to extensive analysis.*

19 **Reply:** Thank you. The comparison of modelled boundary layer depth with observations based
20 on sodar measurements presented in Gallée et al. (2015) was possible on a few days only during
21 the OPALE campaign (see also reply to a similar reviewer comment to Gallée et al. (2015)). NO_x
22 concentrations were measured from 23 November 2011 to 12 January 2012 (this work), HONO from
23 4 December 2011 to 11 January 2012 (Legrand et al., 2014), HO_x radicals from 19 December 2011
24 to 9 January 2012 (Kukui et al., 2014), and CH₂O from 14 December 2011 to 11 January 2012
25 (Preunkert et al., 2014). However, sodar measurements were only available on 12, 13, 18, 21, 26, 27,
26 28 December 2011 and on 3, 4 and 10 January 2012. The best period to compare the MAR model
27 with sodar measurements was 26 to 28 December 2011, because it was the longest Period and also
28 included all chemical trace gases targeted during OPALE.

29 Regarding NO_x observations, additional modelled and observed BL heights were available only
30 during Period III. (9-22 December 2011), which we'll note in the manuscript. Unfortunately, the NO_x
31 vertical profiles measured on 9 January 2012 can only be compared to modelled BL heights due to
32 the lack of sodar data.

33 **Revised text 31298, Lines 8-13:** The strong increase of NO_x around 11 December 2011 falls into a
34 Period when F_{NO_x} almost tripled, while wind speeds slightly decreased and shallow boundary layer
35 heights prevailed with daily h_z maxima below 100-200 m (Fig.1, Table 2). On 12 December and 13
36 December the modelled diurnal ranges of h_z were 3.4-224 m and 3.6-251 m, respectively, while sodar
37 observations yielded 10-150 m and 5-125 m, respectively (Gallée et al., 2015). After 13 December
38 2011 F_{NO_x} remained at high values, thus, the decrease of NO_x mixing ratios appears to be primarily
39 caused by stronger upward mixing into a larger volume, i.e. wind speeds increased and daily h_z
40 maxima grew, exceeding 600 m on 18 December (Fig. 1).

41
42 *Specific:*

43 *Abstract: Should be more specific about the difference between the South Pole and Concordia: It is
44 not just the diurnal cycle but the sudden collapse of the boundary layer in the evening that is unique
45 to Concordia (when the surface flux of NO_x is suddenly confined to a shallow layer).*

46 **Revised text 31283, Lines 5-7:** Profiles of NO_x mixing ratios of the lower 100 m of the atmosphere
47 confirm that, in contrast to South Pole, air chemistry at Dome C is strongly influenced by large diur-
48 nal cycles in solar irradiance and a sudden collapse of the atmospheric boundary layer in the early
49 evening.

50
51 *31284, Lines 15-19: You list four factors leading to high NO_x at the South Pole (Davis et al. 2008)
52 in the introduction. Your conclusion should come back and summarize which of these are relevant to
53 Concordia. In particular, the statement low temperatures leading to low primary production rates of*

54 *HO_x Radicals should be addressed insofar as Davis et al argue that this is what contributes to the*
55 *non-linear increase in the lifetime of NO_x and high accumulation levels at the South Pole is there any*
56 *relevance to the chemistry at Concordia.*

57 **Reply:** Note reply and revised text have been updated compared to the version posted online in
58 **ACPD** The flux values observed at Dome C are typically large enough to explain the average increase
59 in mixing ratios in the early evening (1700-1800 LT). For example in 2009-10 estimated net production
60 rates of NO_x at night are on the order of 100 pptv/h and are consistent with the average increase in
61 NO_x from 110 to 300 pptv over about 2 h from 1700 to 1900 LT (Frey et al., 2013). Similarly in 2011-
62 12 observed increases in NO_x mixing ratios are consistent with NO_x production rates estimated with
63 a simple box model. It is therefore in general not necessary to invoke non-linear HO_x-NO_x chemistry
64 and associated increase in NO_x lifetime as suggested in the case of South Pole (Davis et al., 2008,
65 and references therein). We updated the text accordingly.

66 **Revised text 31299, after Line 2:** Previously, non-linear HO_x-NO_x chemistry and the associated
67 increase in NO_x lifetime were suggested to be an additional factor needed to explain large increases
68 in NO mixing ratios observed at South Pole (Davis et al., 2008, and references therein). In order
69 to assess the relevance of this factor at Dome C we apply a simple box model to estimate net NO_x
70 production rates as done previously (Frey et al., 2013). It is assumed that that mixing is uniform and
71 instantaneous, that the snow emission flux F_{NO_x} is the main NO_x source and the reaction with the
72 OH radical is the dominant NO_x sink.

$$\frac{d[NO_x]}{dt} \sim \frac{F_{NO_x}}{h_z} - k[NO_2][OH] \quad (1)$$

73 where k is the respective reaction rate coefficient. In 2009–10 no OH observations were available
74 at Dome C and average values from South Pole were used instead. In 2009–10 estimated net pro-
75 duction rates of NO_x at night were on the order of 100 pptv/h and therefore explained the observed
76 average increase in NO_x from 110 to 300 pptv over about 2 h from 1700 to 1900 LT (Frey et al., 2013).
77 In 2011-12 the same analysis is repeated using OH measurements available for most of Period IV.
78 (Kukui et al., 2014) as well as h_z calculated with the MAR model (Gallée et al., 2015). Resulting
79 night time values of net NO_x production rates are with about 40 pptv/hr smaller than in 2009-10 but
80 again to a first order consistent with a smaller observed increase in NO_x mixing ratios in the evening
81 hours; i.e. during Period IV. median NO_x increased between 1630 and 1930 LT from 114 to 242 pptv
82 (Fig.6a,f). The above model is oversimplified as the very likely presence of HO₂NO₂ will modulate the
83 diurnal variability of NO_x sinks and sources with an impact on NO_x lifetime as suggested by Davis
84 et al. (2008). However without any information on the diurnal cycle of HO₂NO₂ at Dome C further
85 modelling is not warranted.

86 **Revised text 31301, after Line 16 (Conclusions):** Large mixing ratios of NO_x at Dome C arise from
87 a combination of several factors: continuous sunlight, large NO_x emissions from surface snow and
88 shallow mixing depths after the evening collapse of the convective boundary layer. Unlike at South
89 Pole it is not necessary to invoke non-linear HO_x-NO_x chemistry to explain increases in NO_x mixing
90 ratios. However, uncertainties remain regarding atmospheric levels of HO₂NO₂ and its impact on
91 NO_x life time being a temporary NO_x reservoir.

92
93 *31284, Line 28: A more current reference using sodar data is: B. Van Dam, D. Helmig, W. Neff, and*
94 *L. Kramer, 2013: Evaluation of Boundary Layer Depth Estimates at Summit Station, Greenland. J.*
95 *Appl. Meteor. Climatol., 52, 23562362. doi:10.1175/JAMC-D-13-055.1*

96 **Reply:** Agreed, we replaced the Cohen et al. (2007) reference with the one above.

97
98 *31290, Lines 11-12: Can you argue that the NO_x flux is constant with time through the collapse of*
99 *the boundary layer. Eliminating 22% of the data when the boundary layer depth is < 10m may be*
100 *problematic if this 22% occurs during the evening transition when NO_x levels get large.*

101 **Reply:** The point raised is unclear. We do not argue that flux is constant with time. To the contrary,
102 we argue that the application of MOST requires that at a given time flux is constant between the two
103 measurement heights (condition (a)). Constant flux can be assumed if the chemical lifetime (τ_{chem})
104 of NO_x is much longer than the turbulent transport time scale (τ_{trans}). This condition is met during

105 OPALE, as detailed in the revised text below.

106 However, modelled mixing heights indicate that the upper inlet is frequently above the surface layer
107 (condition (c)) during and after the collapse of the convective BL, as pointed out by the reviewer. Thus
108 the removal of flux estimates (22% of the total available) affects mostly the evening and night, when
109 the BL is shallow. Hence, fluxes during night time are less well constrained, but nevertheless support
110 a significant diurnal cycle (see Figure 6b,g and Figure 9 in Frey et al. (2013)). We clarify this point in
111 the revised text.

112 **Revised text 31290, Lines 8-17:** Condition (a) is met in the surface layer if the chemical lifetime
113 τ_{chem} of NO_x is much longer than the turbulent transport time scale τ_{trans} . Based on observed OH
114 and HO_2 τ_{chem} for NO_x is estimated to be 3 h at 1200 LT and 7 h at 0000 LT during OPALE (Legrand
115 et al., 2014). Estimating τ_{trans} following the approach described previously (Eq. 6 and 7 in Frey et al.,
116 2013) yields 0.6, 1.7 and 2.5 min during the day (0900-1700 LT), the typical time of BL collapse (1700-
117 1900 LT) and during the night (1900-0900 LT), respectively. Thus, τ_{chem} exceeds τ_{trans} by at least a
118 factor 100, confirming that vertical mixing always dominates over the gas phase photochemical sink
119 and flux can be assumed constant between the two inlets. Condition (b) is met as discussed in Frey
120 et al. (2013). For (c) the upper inlet height of 1 m is compared to estimates of mixing height h_z from
121 the MAR model (Gallée et al., 2015). Calculated flux values of NO_x were removed when $h_z < 10\text{m}$
122 resulting in the removal of 22% (773 values) of all available 10 min flux averages. Flux estimates are
123 removed specifically during the evening and night, when the BL is shallow. Hence, fluxes during night
124 time are less well constrained, but nevertheless support a significant diurnal cycle (see Figure 6b,g
125 and Figure 9 in Frey et al. (2013))

126

127 *31293, Lines 10-19: This description of changes in NO_x levels could use a bit more work. The*
128 *intraseasonal trend should be characterized as intraseasonal variability.*

129 **Reply:** As suggested we now characterise in the text the 'trend' as intra-seasonal variability.

130

131 *31293, Lines 10-19 (continued): Also, there is a gap in wind data Dec 3-7. I looked at the AWS*
132 *data (<ftp://amrc.ssec.wisc.edu/pub/aws/10min/rdr/2011/089891211.r>) for this Period and it looks like*
133 *the wind speed was greater in Period II compared to Period III. The AWS anemometer data shows*
134 *frequent stalling in Period III. However, a simple average yields Period II: 2.4 m/s whereas Period III:*
135 *1.3 m/s. This suggests a closer look at the depth of mixing between the two Periods.*

136 **Reply:** Indeed, the statistics for Periods I-IV listed already in Table 2 indicate that wind speeds at
137 3.3 m were greater during Period II (median 3.6 m/s) than during Period III (median 2.5 m/s). We
138 closed the gap in wind data Dec 3-7 using measurements at 2.0m height from the AWS managed by
139 Univ. of Wisconsin, which reduces the median wind speeds during Period II to 3.0 m/s. Recalculating
140 the average wind speeds from the Wisconsin AWS yields 2.98 and 2.34 m/s for Periods II and III,
141 respectively, higher values but with a smaller difference than suggested by the reviewer. Thus, wind
142 speeds in the two Periods are different, but not by much. The primary change driving the increase
143 of NO_x mixing ratios is the increase in flux combined with lower wind speeds and a relatively shallow
144 BL (see above for revised text 31298, Lines 8-13).

145 **Revised Table 2 and Fig. 1:** Median wind speed for Period II updated to 3.0 m/s and Fig. 1 includes
146 now wind speed observations during 3-7 December.

147

148 *31293, Lines 10-19 (continued): With respect to the correlation between wind speed and NO_x levels,*
149 *another factor to look at is the response of NO_x concentrations to the sudden collapse of the boundary*
150 *layer in the evening. Ideally, one should compare average winds during just the Period of collapse*
151 *and higher NO_x: the correlation might come out differently.*

152 **Reply:** Regarding wind speeds, we looked at the correlation with NO_x mixing ratios during the time
153 of collapse of the daytime convective BL, i.e. 1700-1900 LT, and find a slightly stronger negative
154 correlation ($R=-0.45$, $p<0.001$) than when including all data ($R=-0.37$, $p<0.001$).

155 **Revised text 31293, Lines 6-9:** As seen previously at Dome C and other locations, NO_x mixing
156 ratios were weakly but significantly anti-correlated with wind speed ($R=-0.37$, $p<0.001$), especially
157 when only the time Period of the daily collapse of the convective boundary layer, i.e. 1700-1900 LT,

158 was considered ($R=-0.45$, $p<0.001$).

159

160 31293, Lines 10-19 (continued): There were also significant changes in the behaviour of the wind
161 direction: Early Period III shows a 180 degree rotation of the wind whereas Period II shows a most
162 consistent wind direction centered from the SE. In Period III, when the wind was rotating from SW to
163 SE to N, could there have been contamination from the station? (Frey et al 2013, Figure 1; also see
164 Gallee this issue, their Figure 3).

165 **Reply:** Wind directions changed during Period III and rotated through northerly directions, potentially
166 carrying contamination from the generator at Concordia station. However, our data filtering efficiently
167 removes any pollution spikes, which typically exceed 10 ppbv of NO_x (see also Frey et al., 2013).
168 The regular appearing diurnal NO_x maxima are clearly linked to the drastic BL decreases in the early
169 evening, including Period III (Fig. 1). To illustrate this point better we updated Fig.1 and include also
170 a time series of wind direction (Fig. 1). In the method section we provide more detail on how we
171 removed NO_x data affected by local air pollution using a filtering method described previously (Frey
172 et al., 2013).

173 **Revised text in section 2.1:** The mean wind direction during the measurement period was from S
174 (176°) with an average speed of 4.0 m s^{-1} (Fig. 1b). During 2.5% of the time winds came from the
175 direction of Concordia station, i.e. the $355\text{-}15^\circ$ sector (see Fig.1 in Frey et al., 2013), carrying po-
176 tentially polluted air from the station power generator to the measurement site. For example, during
177 Period III winds rotated 4 times through northerly directions (Fig. 1b). Pollution spikes in the raw 1-s
178 data typically exceeded 10 ppbv of NO_x and were effectively removed before computing the 1-min
179 averages by applying a moving 1-min standard deviation filter. Observations were rejected when $1\text{-}\sigma$
180 of NO and NO_2 mixing ratios within a 1-min window exceeded 24 and 90 ppt, respectively.

181

182 *Figure 2: The discussion of this figure might want to include a reference to Argentini et al. 2013*
183 *(Annals of Geophysics 56, 5, 2013; 10.4401/ag-6347) which shows the negative heat flux at sunset*
184 *as well as the decrease in downward longwave radiation for 9 January 2012 (rapid cooling of the*
185 *surface resulting in a strong shallow surface inversion. That paper also shows fairly graphically, using*
186 *sodar data, the evolution of the boundary layer on 10 January 2012 it would be nice to have a similar*
187 *figure for the 9th together with Gallees simulation (note that the Gallee paper in this special issue*
188 *compares modeled versus sodar observed BLD for 26-28 December 2011) It would be nice if these*
189 *comparisons could be coordinated and cross referenced between the papers (e.g. the high NO_x*
190 *Period 12-16 December). Also, Gallees Figure 6 shows a later falloff in BLD in his model than does*
191 *the sodar does the same result hold for the 9th.*

192 **Reply:** In the discussion of Fig.2 we now include a reference to the observations reported in Argentini
193 et al. (2014). As mentioned above in the reply to the first comment, a comparison with modelled
194 and observed BL heights is possible only during a few days of the OPAL campaign. In particular,
195 no sodar data are available for 9 January 2012 and therefore we compare measured NO_x vertical
196 profiles only to modelled BL heights.

197 **Added text in section 3.2; 31294, after Line 12 :** At Dome C rapid cooling of the surface in the
198 evening results in a strong shallow surface inversion (e.g. Frey et al., 2013), and is illustrated by a
199 decrease in downward long-wave radiation and a negative heat flux, as observed in the evening of 9
200 January 2012 (Fig.4 in Argentini et al., 2014).

201

202 *Section 3.5.2, : This section should probably reference/compare other NOX flux measurements. See*
203 *Davis et al 2008 and references therein (Onckley et al, Wolff eta al., Wang et al. and Neff et al) that*
204 *discuss the magnitudes, estimates, and boundary depth effects relevant to the NOX flux (esp. Wang*
205 *et al).*

206 **Reply:** As suggested we expand the discussion referring to previous estimates of NO_x emission flux
207 (F_{NO_x}) from polar snow based on observations and models.

208 **Added text in section 3.5.2; 31294, before Line 1:** The NO_x flux observed above polar snow
209 is on the order of 10^{12} to 10^{13} molecule $\text{m}^{-2} \text{ s}^{-1}$ and contributes significantly to the NO_x budget
210 in the polar boundary layer. At the lower end of the range are F_{NO_x} observations at Summit,

211 Greenland (Honrath et al., 2002) and at Neumayer in coastal Antarctica (Jones et al., 2001) with
212 2.5×10^{12} molecule $m^{-2} s^{-1}$, whereas on the Antarctic Plateau F_{NO_x} values are up to ten times larger
213 (Oncley et al., 2004; Frey et al., 2013, and this study). The average F_{NO_x} at South Pole during 26-30
214 November 2000 was 3.9×10^{12} molecule $m^{-2} s^{-1}$ (Oncley et al., 2004), whereas at Dome C observed
215 fluxes are 2-6 times larger, with seasonal averages of $8-25 \times 10^{12}$ molecule $m^{-2} s^{-1}$ (Frey et al., 2013,
216 this work). Due to the uncertainties in the processes leading to NO_x production it had been difficult
217 to explain inter-site differences, e.g. by simply scaling F_{NO_x} with UV irradiance and nitrate in the
218 surface snow pack (Davis et al., 2004). Some of the variability in flux values may be due to differ-
219 ences in experimental set up or in the employed flux estimation method (e.g. Davis et al., 2004; Frey
220 et al., 2013). For example, the F_{NO_x} estimates for South Pole are based on measured NO gradients
221 only, inferring NO_x from photochemical equilibrium and using the Bowen ratio method (Oncley et al.,
222 2004), whereas the F_{NO_x} estimates for Dome C are based on observations of both atmospheric ni-
223 trogen oxides (NO and NO_2) and the flux-gradient method (Frey et al., 2013).
224 Model predictions of F_{NO_x} show in general a low bias on the Antarctic Plateau when compared to
225 observations. A first 3-D model study for Antarctica included NO_x snow emissions parameterised
226 as a function of temperature and wind speed to match the observed F_{NO_x} at South Pole (Wang
227 et al., 2007). However, the model under-predicts NO mixing ratios observed above the wider Antarc-
228 tic Plateau highlighting that the model lacks detail regarding the processes driving the emission flux
229 (Wang et al., 2007). The first model study to calculate F_{NO_x} based on NO_3^- photolysis in snow, as
230 described in this work, reports $1-1.5 \times 10^{12}$ molecule $m^{-2} s^{-1}$ for South Pole in summer (Wolff et al.,
231 2002), about a factor 4 smaller than the observations by Oncley et al. (2004) and up to 16 times
232 smaller than what is needed to explain rapid increases in NO_x mixing ratios over a few hours (Davis
233 et al., 2008, and references therein). Recent model improvements reduced the mismatch with the
234 South Pole flux observations and included the use of updated absorption cross sections and quan-
235 tum yield of the nitrate ion, as well as e-folding depths measured in surface snow on the Antarctic
236 Plateau, and resulted in a factor 3 increase of flux calculated for South Pole (France et al., 2011).
237 In light of major remaining uncertainties, which include the spatial variability of nitrate in snow and
238 the quantum yield of nitrate photolysis (Frey et al., 2013), we discuss below the variability of F_{NO_x}
239 observed at Dome C.
240

241 References

- 242 Argentini, S., Petenko, I., Viola, A., Mastrantonio, G., Pietroni, I., Casasanta, G., Aristidi, E., and
243 Genthon, C.: The surface layer observed by a high-resolution sodar at DOME C, Antarctica, *Annals*
244 *of Geophysics*, 56, 1–10, doi:10.4401/ag-6347, 2014.
- 245 Bauguitte, S. J.-B., Bloss, W. J., Evans, M. J., Salmon, R. A., Anderson, P. S., Jones, A. E., Lee, J. D.,
246 Saiz-Lopez, A., Roscoe, H. K., Wolff, E. W., and Plane, J. M. C.: Summertime NO_x measurements
247 during the CHABLIS campaign: can source and sink estimates unravel observed diurnal cycles?,
248 *Atmos. Chem. Phys.*, 12(2), 989–1002, doi:10.5194/acp-12-989-2012, 2012.
- 249 Davis, D. D., Seelig, J., Huey, G., Crawford, J., Chen, G., Wang, Y. H., Buhr, M., Helmig, D., Neff,
250 W., Blake, D., Arimoto, R., and Eisele, F.: A reassessment of Antarctic plateau reactive nitrogen
251 based on ANTCI 2003 airborne and ground based measurements, *Atmos. Environ.*, 42, 2831–
252 2848, doi:10.1016/j.atmosenv.2007.07.039, 2008.
- 253 Davis, D. D., Chen, G., Buhr, M., Crawford, J., Lenschow, D., Lefter, B., Shetter, R., Eisele, F., Mauldin,
254 L., and Hogan, A.: South Pole NO_x chemistry : an assessment of factors controlling variability and
255 absolute levels, *Atmos. Environ.*, 38(32), 5275–5388, doi:10.1016/j.atmosenv.2004.04.039, 2004.
- 256 France, J. L., King, M. D., Frey, M. M., Erbland, J., Picard, G., Preunkert, S., MacArthur, A., and
257 Savarino, J.: Snow optical properties at Dome C (Concordia), Antarctica; implications for snow
258 emissions and snow chemistry of reactive nitrogen, *Atmos. Chem. Phys.*, 11(18), 9787–9801,
259 doi:10.5194/acp-11-9787-2011, 2011.
- 260 Frey, M. M., Brough, N., France, J. L., Anderson, P. S., Traulle, O., King, M. D., Jones, A. E.,
261 Wolff, E. W., and Savarino, J.: The diurnal variability of atmospheric nitrogen oxides (NO and NO_2)

262 above the Antarctic Plateau driven by atmospheric stability and snow emissions, *Atmos. Chem.*
263 *Phys.*, 13, 3045–3062, doi:10.5194/acp-13-3045-2013, 2013.

264 Gallée, H., Preunkert, S., Argentini, S., Frey, M. M., Genthon, C., Jourdain, B., Pietroni, I., Casasanta,
265 G., Barral, H., Vignon, E., Amory, C., and Legrand, M.: Characterization of the boundary layer at
266 Dome C (East Antarctica) during the OPALE summer campaign, *Atmos. Chem. Phys.*, 15, 6225–
267 6236, doi:10.5194/acp-15-6225-2015, 2015.

268 Honrath, R., Lu, Y., Peterson, M., Dibb, J., Arsenault, M., Cullen, N., and Steffen, K.: Vertical fluxes of
269 NO_x, HONO, and HNO₃ above the snowpack at Summit, Greenland, *Atmos. Environ.*, 36, 2629–
270 2640, doi:10.1016/S1352-2310(02)00132-2, 2002.

271 Jones, A. E., Weller, R., Anderson, P. S., Jacobi, H. W., Wolff, E. W., Schrems, O., and Miller, H.:
272 Measurements of NO_x emissions from the Antarctic snow pack, *Geophys. Res. Lett.*, 28(8), 1499–
273 1502, 2001.

274 Kukui, A., Legrand, M., Preunkert, S., Frey, M. M., Loisil, R., Gil Roca, J., Jourdain, B., King, M. D.,
275 France, J. L., and Ancellet, G.: Measurements of OH and RO₂ radicals at Dome C, East Antarctica,
276 *Atmos. Chem. Phys.*, 14, 12373–12392, doi:10.5194/acp-14-12373-2014, 2014.

277 Legrand, M., Preunkert, S., Frey, M., Bartels-Rausch, Th., Kukui, A., King, M. D., Savarino, J., Ker-
278 brat, M., and Jourdain, B.: Large mixing ratios of atmospheric nitrous acid (HONO) at Concordia
279 (East Antarctic Plateau) in summer: a strong source from surface snow?, *Atmos. Chem. Phys.*, 14,
280 9963–9976, doi:10.5194/acp-14-9963-2014, 2014.

281 Oncley, S. P., Buhr, M., Lenschow, D. H., Davis, D., and Semmer, S. R.: Observations of summertime
282 NO fluxes and boundary-layer height at the South Pole during ISCAT 2000 using scalar similarity,
283 *Atmos. Environ.*, 38(32), 5389–5398, doi:10.1016/j.atmosenv.2004.05.053, 2004.

284 Preunkert, S., Legrand, M., Frey, M., Kukui, A., Savarino, J., Gallée, H., King, M., Jourdain, B., Vicars,
285 W., and Helmig, D.: Formaldehyde (HCHO) in air, snow and interstitial air at Concordia (East
286 Antarctic plateau) in summer, *Atmos. Chem. Phys. Disc.*, 14, 32027–32070, doi:10.5194/acpd-14-
287 32027-2014, 2014.

288 Wang, Y. H., Choi, J., Zeng, T., Davis, D., Buhr, M., Huey, G., and Neff, W.: Assessing the photo-
289 chemical impact of snow NO_x emissions over Antarctica during ANTCTI 2003, *Atmos. Environ.*, 41,
290 3944–3958, 2007.

291 Wolff, E. W., Jones, A. E., Martin, T. J., and Grenfell, T. C.: Modelling photochemical NO_x pro-
292 duction and nitrate loss in the upper snowpack of Antarctica, *Geophys. Res. Lett.*, 29(20),
293 doi:10.1029/2002GL015823, 2002.

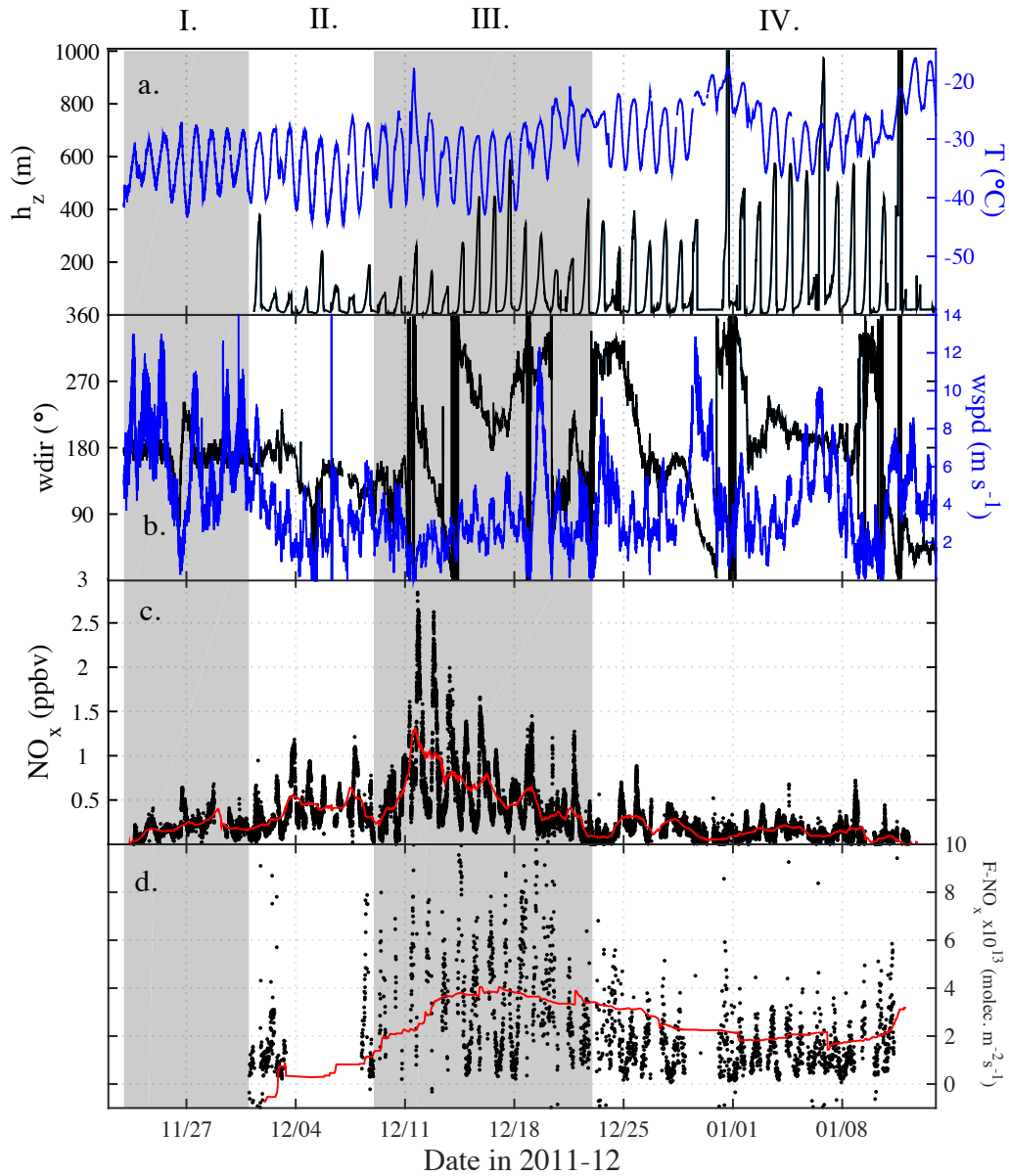


Figure 1: Meteorology and NO_x observations at Dome C in summer 2011–2012 (highlighted Periods I.–IV. as referred to in text and Table 2): **(a)** air temperature (T) at 1.6m and modeled mixing height (h_z) (Gallée et al., 2015), **(b)** wind speed (wspd) and direction (wdir) at 3.3 m **(c)**, 1 min averages of NO_x mixing ratios at 1 m (red line is 1 day running mean) and **(d)** 10 min averages of observational estimates of NO_x flux (F_{NO_x}) between 0.01 and 1 m (red line is 14 day running mean).

1 **Reply to comments of Referee No.2**

2 We thank Referee No.2 for insightful comments which helped to further improve the manuscript. Ref-
3 eree comments (in italics) are addressed below. Revised text, keyed to the ACPD online version, is
4 shown in blue, and is included in the final manuscript we will submit to ACP.

5
6 *This manuscript focuses on observations of NO and NO₂ from 10 cm into the firn up to 100 m above
7 the snow surface, and measurement of the flux of NO_x (primarily) out of the snow, made at Dome
8 C during the OPAL campaign. There were abundant supporting measurements available, allowing
9 the authors to put important constraints on the factors controlling variations in the mixing ratios of
10 the nitrogen oxides and the snow to air flux of NO_x over a range of time scales. At Dome C it is
11 clear that the interplay between the strength of the snow source of NO_x and vertical mixing exerts
12 primary control over the mixing ratio of NO_x, both over the course of a day and a season. To first
13 order, the strength of the snow source can also be explained as a combination of the abundance of
14 NO₃⁻ in the snow available for photolysis and the actinic flux in the 300-340 nm range. However, it
15 is evident that variations in the strength of the snow source of NO_x depend on additional factors that
16 are not fully understood. Authors suggest that the fraction of NO₃⁻ readily photolyzed can change,
17 both within a single season and between years, and suggest more field, lab and model studies are
18 needed to understand what makes some NO₃⁻ - photo-labile while other NO₃⁻ is not. The latter fraction
19 is tentatively labeled photo-stabile, I suggest that we do not need a new word and that photo-stable
20 or just stable should be adequate terminology.*

21 **Reply:** We replaced photo-stabile with photo-stable in the text.

22
23 *In general, the results are clearly presented, and the arguments supporting conclusions are well
24 laid out. I will suggest a few places where I feel that clarity could be improved in the list of detailed
25 minor comments below. However, I feel that more detail is needed in the description of methods. Most
26 importantly, the authors need to explain how the concentration gradients were measured. Seems that
27 the 2-channel CLD allowed NO and NO_x (and something like NO₂ by difference) to be determined
28 simultaneously, but only one inlet could be sampled at a time. So, what was the cycle between
29 0.1, 1.0 and 4.0 m sampling heights? How much of each 10 minute interval was spent at each
30 height? Was each height measured several times in the 10 minutes, or was it 0-3.333 minutes on
31 one inlet, 3.333-6.666 on next and then 6.666-10 on the third? One presumes that there had to be
32 some down time for zeroing and calibration, perhaps quite frequently, so did these essential intervals
33 of housekeeping result in gaps during all or most 10-minute gradient measurements, or were they
34 grouped into a longer period of no data once or several times each day?*

35 **Reply:** The measurement method as well as the duty cycle of the CLD during the gradient measure-
36 ments were described previously in Frey et al. (2013). However, we repeat some of the requested
37 details in the methods section.

38 **Revised text 31287, after Line 17:** The three sample inlets were connected inside the lab shelter to
39 a valve box, which automatically switched the CLD between sampling heights on a 90 s duty cycle.
40 As described below, the 10-minute average concentration difference ΔNO_x between the 0.01 and 1.0
41 m inlets is used to estimate flux. Therefore, 10-minute mean ΔNO_x values are calculated on average
42 from two sets of two subsequent 90 s intervals, separated by a 90 s interval during which the 4.0 m
43 inlet was measured. Baseline count rates were determined by adding excess ozone to sample air
44 in a pre-chamber so that all electronically excited NO₂ has returned to ground state when reaching
45 the reaction chamber. The baseline was measured for 60 s every 13.5 min alternating between all
46 three inlets. The NO sensitivity of the CLDs was determined every 14 h by standard addition to the
47 sample air matrix of a 1 ppm NO/NO₂ mixture (UK National Physics Laboratory traceable BOC cer-
48 tified), which is further diluted to 4 ppbv of NO. During standard runs also the conversion efficiency
49 (CE) of the photolytic converter was determined by addition of a known mole fraction of NO₂. This
50 was achieved by gas phase titration of the NO/NO₂ mixture to NO₂ by O₃ generated from a pen-ray
51 lamp, and monitoring the un-titrated NO mole fraction. The instrument artefact originating from NO_x
52 producing surface reactions in inlets and reaction cells was determined by overflowing the instrument
53 inlet with scrubbed ambient air supplied by a pure air generator (Eco-Physics PAG003). The artefact

54 was measured every 14 h, offset by 7 h to the calibration runs.

55

56 *I also feel that more detail needs to be provided regarding the measurements of snow nitrate in the*
57 *field lab. It is stated that samples were collected every few days, but I am curious if they were analyzed*
58 *right after collection (that day or the next), or allowed to pile up and then run in larger batches several*
59 *times through the season, or maybe even all in one bunch near the end (this last option might be*
60 *the best answer, but seems unlikely). In general, this would not seem something to worry about*
61 *except for the fact that Berhanu et al. also have a manuscript on OPALE in review at ACPD right now,*
62 *and indicate some uncertainty about nitrate measurements at Dome C during the 2011-12 season.*
63 *Specifically, they measured what was supposed to be the same snow in 2 different artificial snow*
64 *pits 12 different times through the season and found a range from 1200-1700 ppb (around a stated*
65 *true value of 1450 ppb). This variability was not seen in samples run in a single batch, rather was*
66 *expressed as large shifts between samples run on different days. Were the samples in present study*
67 *and those reported by Berhanu et al. all run by same technician on the same instrument (commingled*
68 *in batches)?*

69 **Reply:** During OPALE the skin layer of surface snow, i.e. the top few mm, was sampled every 3 days.
70 Samples were stored together with the additional snow samples discussed in Berhanu et al. (2014)
71 and then analysed for nitrate in batches by the same operator. There has been a systematic shift in
72 the nitrate standard response in between individual batch runs due to a calibration issue, which may
73 affect the time series of nitrate in surface snow (Berhanu et al., 2014). However we believe the trend
74 during Period II and III (Fig.7c) is real for two reasons: a) all samples were analysed in random order,
75 across several batches, but the temporal trend observed in surface snow concentrations is very sim-
76 ilar in both the skin layer (top few mm) and in the top layer of adjacent snow pits (top 2cm) (Fig.4 in
77 Berhanu et al., 2014). And b) nitrate maxima in Antarctic surface snow during summer are a robust
78 feature observed at Dome C over the existing 2009-present period of year-round sampling (Fig. 7b
79 shows 2011-12 and 2009-10), as well as in coastal Antarctica (e.g. Mulvaney et al., 1998). Thus the
80 snow nitrate changes over a week with a typical amplitude of 800-1000 ppbw are repeatable and well
81 above the spatial variability of 20-25% found at Dome C (France et al., 2011; Frey et al., 2013). See
82 revised text further below.

83

84 *How much would modeled NO_x fluxes change if snow nitrate was adjusted up or down by nearly*
85 *20%?*

86 **Reply:** The NO_x emission flux scales with nitrate concentrations in snow as illustrated by equation 3,
87 and therefore an uncertainty of 20-25% in nitrate concentration, which is in fact typical for the spatial
88 variability seen at Dome C, will translate to a similar variability in F_{NO_x} (see Fig.7c and discussion in
89 Frey et al., 2013).

90

91 *Are the higher values of skin nitrate in periods II and III in 2011-12 real, or related to standard drift*
92 *(sensu Berhanu et al.)?*

93 **Reply:** As discussed above the higher values during Period II and III represent in our opinion a real
94 temporal trend.

95

96 *Are the surface snow data in Fig. 7 of this manuscript the same as those in Fig 4 of Berhanu (seem*
97 *similar, but maybe not identical)? At a minimum, authors need to make a good faith estimate of the*
98 *precision and accuracy of their own snow nitrate concentrations given the apparent problems in the*
99 *field during OPALE.*

100 **Reply:** The nitrate concentrations in the skin layer of surface snow during 2011-12 used in this work
101 (Fig.7b) are the same as presented in Fig.4 of Berhanu et al. (2014). The updated precision is 5%
102 based on replicate standard measurements (see also reply to reviewer No.1 in the online discussion
103 of Berhanu et al. (2014)). The overall accuracy including systematic errors in calibration and collec-
104 tion of just the top few mm of snow is of the order of 20%, comparable to the spatial variability of
105 nitrate in surface snow at Dome C.

106

107 **Revised text 31292, after Line 3:** Samples were stored together with the additional snow samples
108 discussed in Berhanu et al. (2014) and then analysed for nitrate in batches by the same operator. The
109 precision is 5% based on replicate standard measurements. Due to a systematic shift in the nitrate
110 standard response in between individual batch runs due to a calibration issue (Berhanu et al., 2014)
111 the accuracy is larger than usual. The overall accuracy including systematic errors in calibration and
112 collection of just the top few mm of snow is of the order of 20%, and is therefore comparable to the
113 spatial variability of nitrate in surface snow at Dome C (France et al., 2011). Note that the temporal
114 trend of nitrate concentrations observed in surface snow discussed below is significantly larger, i.e.
115 >50%.

116
117 *Specific, mostly minor, comments keyed to line numbers in 9 Nov 14 Latex file.*

118
119 *11 interference by pernitric* **Reply:** Done.

120
121 *21-22 last sentence of abstract seems to clash with the one just before, and kind of comes out of*
122 *the blue. Paper does develop this idea, but maybe it should just be in conclusions (or it needs to be*
123 *brought into abstract less abruptly.*

124 **Revised text 31283, Lines 23-24:** A remaining source of uncertainty and subject of future research
125 is the quantum yield of nitrate photolysis in natural snow, which may change over time as the snow
126 ages.

127
128 *61 do not need mixing ratios and levels both in this sentence* **Reply:** Corrected.

129
130 *72-74 agreed that the quantum yield uncertainty is important, but probably not the dominant problem*
131 *models are facing. Seems premature to highlight this again here.* **Reply:** We removed this sentence.

132
133 *104-105 only air from the bottom and sides could enter through small holes in the tube (might help to*
134 *specify that the holes were x cm or mm above the bottom of the probe)*

135 **Revised text 31287, Line 6:** ... from the bottom and sides could enter, using small horizontal holes
136 at 0-10 cm above the bottom of the tube.

137
138 *116 CLD employed also converts nitrous* **Reply:** Done.

139
140 *126-158 to me, it would flow more smoothly to switch the order of these 2 paragraphs, dealing with*
141 *possible HNO₄ artifact on the NO₂ measurement right after HONO/NO. Then talk about how both*
142 *possible problems and any vertical gradients might impact the NO_x gradients.*

143 **Reply:** Agreed, and we changed the order.

144
145 *187 given how important mixing height is for much of the discussion, I would like to see some indi-*
146 *cation that MAR has been validated. Ideally at DOME C (from tower, tether sonde, maybe aircraft*
147 *profiles) but at least from somewhere on the Antarctic plateau.*

148 **Revised text 31290, Line 10:** The MAR model has been validated previously over the Antarctic
149 Plateau, focusing on Dome C, during winter (Gallée and Gorodetskaya, 2010) and now also during
150 summer (Gallée et al., 2014).

151
152 *Equation 3, might mention that this model probably estimates an upper limit for NO₂ flux (if the*
153 *quantum yield and actinic flux are correct) since it assumes all NO₂ formed escapes the firn before*
154 *any of it can photolyze, or convert to HNO₃, HONO, HNO₄.*

155 **Revised text 31292, after Line 24:** For the discussion below it should be borne in mind that the
156 calculated F_{NO_2} is a potential emission flux assuming that NO₂ is vented immediately after release
157 from the snow grain to the air above the snow pack without undergoing any secondary reactions.

158
159 *265 intra-seasonal trend odd terminology, since it seems you are talking about the week long period*

160 *with enhanced mixing ratios, not really a trend through the 2 months*

161 **Reply:** We replaced Intra-seasonal trend by "intra-seasonal variability" throughout the text.

162

163 *268-269 to late December average (not Nov)*

164 **Reply:** We clarify this.

165 **Revised text 31293, Lines 15-16:** After that NO_x mixing ratios gradually dropped over 10 days (Pe-
166 riod III-IV) to median concentrations of ~120 pptv, slightly lower than observed in late November
167 (Table 2).

168

169 *270 2.5 times that* **Reply:** Done.

170

171 *273 median (range) of 1.6 (0.4-2.9) this is a little misleading. The range shown in Fig 1 D is -1 to 10*
172 *x 10¹³. The smaller range in the text comes from Table 1 which compares season long medians for*
173 *noon and midnight.*

174 **Reply:** We believe to assess the range of flux values it is a more conservative measure to state
175 median values at noon and midnight, which are less sensitive to extreme values and the occasional
176 outlier present in relatively noisy flux estimates. We clarify this.

177 **Revised text 31293, Lines 21:**... with a median of 1.6×10^{13} molecule $m^{-2} s^{-1}$. Median values of
178 F_{NO_x} at midnight and at noon were 0.4 and 2.9×10^{13} molecule $m^{-2} s^{-1}$, respectively (Table 1).

179

180 *276 almost 5 times (or, about 4.7 times)* **Revised text 31293, Lines 24:** almost 5 times

181

182 *305-309 Any speculation about why the nitrate profile in the pit under the disk so much different than*
183 *away from all the activity?*

184 **Reply:** We have no definite answer to this question. The firn air probe was installed onto untouched
185 snow, and only removed after the end of the atmospheric sampling period. Thus contamination is
186 unlikely, but a local anomaly remains a possibility as pits 5m next to the lab shelter showed a similar
187 increase of concentration with depth.

188 **Revised text 31295, Line 5:** The firn air probe was installed onto untouched snow, and only removed
189 after the end of the atmospheric sampling period. Thus contamination due to local activity appears
190 unlikely, but a local anomaly remains a possibility as snow pits 5 m next to the lab shelter showed a
191 similar increase of concentration with depth (data not shown).

192

193 *316 the anticorrelation between NO₂ and O₃ is interesting, but the suggestion that it reflects enhanced*
194 *nitrate in the snow is not supported. Profile in P3 does not get so deep and neither of the other pits*
195 *shows a peak near 45 cm.*

196 **Revised text 31295, Line 11-13:** In particular, the drop of O₃ mixing ratios by >10ppbv at 45 cm
197 depth was not an outlier since collocated NO₂ mixing ratios were also significantly elevated compared
198 to adjacent snow layers. However, no snow nitrate measurements were available to further investi-
199 gate the origin of the NO₂ peak.

200

201 *351-354 seems the details of the MAX DOAS data reduction should have been in Methods*

202 **Reply:** We moved this part to the method section.

203

204 *370-371 this statement begs for at least a back of the envelope attempt at quantification. You earlier*
205 *estimated that HNO₄ might contribute 33-66 ppt artifact to NO₂, so what would happen if you reduced*
206 *NO₂ by this much in the steady state calculation? Hard to believe this would account for much of the*
207 *factor of 20 discrepancy.*

208 **Reply:** This is a very useful comment. In reassessing the potential HNO₄ interference we discovered
209 a computational error, which reduces the estimated magnitude of the HNO₄ interference by a factor
210 two. NO₂ mixing ratios are corrected, assuming that additional NO₂ is measured in the CLD from
211 HNO₄ thermal decomposition, equivalent to 25% of ambient HNO₄ on the order of 130 pptv. We find
212 that average steady-state estimates of oxidant concentrations are still a factor 10 larger than those

213 observed (RO_2 and BrO). In the revised text we take this into account and put the role of HNO_4 as an
214 interferent into perspective.

215

216 **Revised text 31288, Line 29:** HNO_4 present at these values could potentially produce 16-32 pptv of
217 NO_2 in the photolytic converter, equivalent to 8-16% of the average NO_2 mixing ratio measured at 1
218 m.

219 **Revised text 31297, Line 9-16:** The same steady-state calculation as described in Frey et al. (2013)
220 was repeated for austral summer 2011-12 and yields an average of 2.5×10^9 molecule cm^{-3} or 129
221 pptv of total radical concentrations $[OX] = [HO_2] + [RO_2] + 2[XO]$. Observations based on median
222 $[RO_2]$ of 9.9×10^7 molecule cm^{-3} or 5 pptv (Kukui et al., 2014) and 3 pptv of BrO yield $[OX]$ of about
223 11 pptv. Hence, the estimated total radical concentration exceeds observations by a factor 12. To
224 estimate the impact of a potential interference by HNO_4 we corrected the NO_2 mixing ratios, assum-
225 ing that additional NO_2 is measured in the CLD from HNO_4 thermal decomposition, equivalent to
226 25% (100%) of ambient HNO_4 on the order of 130 pptv. We then find that the average steady-state
227 estimate of oxidant concentrations is still a factor 10 (3) larger than those observed. Thus, a least a
228 part of the inconsistency may be explained by the interference with HNO_4 (not measured).

229

230 375-385 this section is a little loose. Starts by saying that period II looks much like 2009-10 with peak
231 18-20:00 but the figure shows that in 2009-10 the peak lasted later into the evening. Indeed, in all
232 of the intervals except II the evening peak lasts quite a bit past 20:00. Why would that be, since the
233 mixing height is not getting much lower, and the snow source should be weakening.

234 **Reply:** Thanks for pointing this out. Indeed, NO_x mixing ratios typically show maxima lasting into the
235 night time hours in 2009-10 and in 2011-12 (except Period II.), whereas NO mixing ratios peak during
236 1800-2000 LT in 2009-10 (Fig.5 in Frey et al., 2013) and in 2011-12 (data not shown). Assuming
237 no significant changes in BL height after the initial collapse of the convective BL night-time peaks of
238 NO_x are plausible if the weakening of snow emissions was offset by a corresponding decrease of the
239 chemical sink of NO_x , i.e. the NO_2+OH reaction. This is consistent to a first order taking into account
240 that observed OH concentrations and F- NO_x vary in a similar way, by up to a factor 5 between local
241 noon and midnight. We revise the text accordingly.

242 **Revised text 31297, Lines 18-28:** On diurnal time scales NO_x mixing ratios at Dome C are con-
243 trolled by the interplay between snowpack source strength and atmospheric physical properties, i.e.
244 turbulent diffusion of heat K_h and mixing height h_z of the boundary layer. The median diurnal cy-
245 cles of NO_x mixing ratios in 2011-12 show with the exception of Period II (1-8 December) previously
246 described behaviour (Frey et al., 2013), with a strong increase around 1800 LT to maximum values,
247 which last into the night time hours (Fig.6a). Night-time peaks of NO_x are plausible if the weakening
248 of snow emissions was offset by a corresponding decrease of the chemical sink of NO_x , i.e. the
249 NO_2+OH reaction, assuming no significant change in h_z . This is consistent to a first order taking into
250 account that observed OH concentrations (Kukui et al., 2014) and F- NO_x vary in a similar way, by up
251 to a factor 5 between local noon and midnight.

252

253 427-436 Another place text could/should be more precise. Assuming the snow nitrate concentrations
254 are valid, the really high levels are only present at the end of II and beginning of III, not through both
255 periods. Cant say much about NO_x flux in II, but it clearly stays high through nearly all of III, despite
256 an apparent steep drop in nitrate.

257

258 **Reply:** We agree and therefore refined the description of the observations in the text accordingly.

259 **Revised text 31299, Lines 21-24:** Instead changes in F_{NO_x} can be linked to the temporal variability
260 present in the snow skin layer. During the end of Period II. and beginning of Period III. skin layer NO_3^-
261 concentrations were up to two times larger than before and after (Fig.7b). F_{NO_x} is high during the
262 end of Period II. and beginning of Period III., however drops off a week after the decrease of nitrate
263 concentrations in surface snow.

264

265 451 corresponds to days of should this be to No of days?

266 **Revised text 31300, Line 18:** *quantum yield ... decreased from 0.44 to 0.003 within what corre-*
267 *sponds to a few days of UV exposure in Antarctica ...*
268
269 452 in quantum yield is **Reply:** Corrected.
270
271 453 dont think stabile is a word and stable would probably work **Reply:** Corrected.
272
273 455 Neff and Davis also advocating for different flavors of nitrate in snow, shown on their poster at
274 AICI CASSI, with references to earlier work.
275 **Reply:** Correct, thus we added a reference to the earlier work by Davis et al. (2008).
276
277 480 is an O3 sink Corrected.
278
279 491-493 as noted earlier, should estimate how big a part HNO₄ might explain **Reply:** See reply above.
280

281 References

- 282 Berhanu, T. A., Savarino, J., Erbland, J., Vicars, W. C., Preunkert, S., Martins, J. F., and Johnson,
283 M. S.: Isotopic effects of nitrate photochemistry in snow: a field study at Dome C, Antarctica,
284 *Atmos. Chem. Phys. Disc.*, 14, 33 045–33 088, doi:10.5194/acpd-14-33045-2014, 2014.
- 285 Davis, D. D., Seelig, J., Huey, G., Crawford, J., Chen, G., Wang, Y. H., Buhr, M., Helmig, D., Neff,
286 W., Blake, D., Arimoto, R., and Eisele, F.: A reassessment of Antarctic plateau reactive nitrogen
287 based on ANTCI 2003 airborne and ground based measurements, *Atmos. Environ.*, 42, 2831–
288 2848, doi:10.1016/j.atmosenv.2007.07.039, 2008.
- 289 France, J. L., King, M. D., Frey, M. M., Erbland, J., Picard, G., Preunkert, S., MacArthur, A., and
290 Savarino, J.: Snow optical properties at Dome C (Concordia), Antarctica; implications for snow
291 emissions and snow chemistry of reactive nitrogen, *Atmos. Chem. Phys.*, 11(18), 9787–9801,
292 doi:10.5194/acp-11-9787-2011, 2011.
- 293 Frey, M. M., Brough, N., France, J. L., Anderson, P. S., Traulle, O., King, M. D., Jones, A. E.,
294 Wolff, E. W., and Savarino, J.: The diurnal variability of atmospheric nitrogen oxides (NO and NO₂)
295 above the Antarctic Plateau driven by atmospheric stability and snow emissions, *Atmos. Chem.*
296 *Phys.*, 13, 3045–3062, doi:10.5194/acp-13-3045-2013, 2013.
- 297 Gallée, H., Preunkert, S., Argentini, S., Frey, M. M., Genthon, C., Jourdain, B., Pietroni, I., Casasanta,
298 G., Barral, H., Vignon, E., and Legrand, M.: Characterization of the boundary layer at Dome C (East
299 Antarctica) during the OPAL summer campaign, *Atmos. Chem. Phys. Disc.*, 14, 33 089–33 116,
300 doi:10.5194/acpd-14-33089-2014, 2014.
- 301 Gallée, H. and Gorodetskaya, I.: Validation of a limited area model over Dome C, Antarctic Plateau,
302 during winter, *Clim. Dynam.*, 34, 61–72, doi:10.1007/s00382-008-0499-y, 2010.
- 303 Kukui, A., Legrand, M., Preunkert, S., Frey, M. M., Loisil, R., Gil Roca, J., Jourdain, B., King, M. D.,
304 France, J. L., and Ancellet, G.: Measurements of OH and RO₂ radicals at Dome C, East Antarctica,
305 *Atmos. Chem. Phys.*, 14, 12 373–12 392, doi:10.5194/acp-14-12373-2014, 2014.
- 306 Legrand, M., Preunkert, S., Frey, M., Bartels-Rausch, Th., Kukui, A., King, M. D., Savarino, J., Ker-
307 brat, M., and Jourdain, B.: Large mixing ratios of atmospheric nitrous acid (HONO) at Concordia
308 (East Antarctic Plateau) in summer: a strong source from surface snow?, *Atmos. Chem. Phys.*, 14,
309 9963–9976, doi:10.5194/acp-14-9963-2014, 2014.
- 310 Mulvaney, R., Wagenbach, D., and Wolff, E. W.: Postdepositional change in snowpack nitrate from
311 observation of year-round near-surface snow in coastal Antarctica, *J. Geophys. Res.*, 103, 11 021–
312 11 031, 1998.

Atmospheric nitrogen oxides (NO and NO₂) at Dome C, East Antarctica, during the OPALE campaign

M. M. Frey¹, H. K. Roscoe¹, A. Kukui^{2,3}, J. Savarino^{4,5}, J. L. France⁶,
M. D. King⁶, M. Legrand^{4,5}, and S. Preunkert^{4,5}

¹British Antarctic Survey, Natural Environment Research Council, Cambridge, UK

²Laboratoire Atmosphère, Milieux et Observations Spatiales (LATMOS), UMR8190, CNRS-Université de Versailles Saint Quentin, Université Pierre et Marie Curie, Paris, France

³Laboratoire de Physique et Chimie de l'Environnement et de l'Éspace (LPC2E), UMR6115 CNRS-Université d'Orléans, 45071 Orléans cedex 2, France

⁴Université Grenoble Alpes, Laboratoire de Glaciologie et Géophysique de l'Environnement (LGGE), 38000 Grenoble, France

⁵CNRS, Laboratoire de Glaciologie et Géophysique de l'Environnement (LGGE), 38000 Grenoble, France

⁶Department of Earth Sciences, Royal Holloway University of London, Egham, Surrey, TW20 0EX, UK

Correspondence to: M. M. Frey (maey@bas.ac.uk)

Abstract

Mixing ratios of the atmospheric nitrogen oxides NO and NO₂ were measured as part of the OPALE (Oxidant Production in Antarctic Lands & Export) campaign at Dome C, East Antarctica (75.1° S, 123.3° E, 3233 m), during December 2011 to January 2012. Profiles of NO_x mixing ratios of the lower 100 m of the atmosphere confirm that, in contrast to South Pole, air chemistry at Dome C is ~~dominated by strong~~ strongly influenced by large diurnal cycles in solar irradiance and atmospheric stability a sudden collapse of the atmospheric boundary layer in the early evening. Depth profiles of mixing ratios in firn air suggest that the upper snowpack at Dome C holds a significant reservoir of photolytically produced NO₂ and is a sink of gas phase ozone (O₃). First-time observations of BrO at Dome C suggest 2–3 pptv near the ground, with higher levels in the free troposphere. Assuming steady-state, observed mixing ratios of BrO and RO₂ radicals are too low to explain the large NO₂ : NO ratios found in ambient air. A ~~previously not considered interference with~~ possible interference by pernitric acid (HO₂NO₂) may explain part of this inconsistency. During 2011–2012 NO_x mixing ratios and flux were larger than in 2009–2010 consistent with also larger surface O₃ mixing ratios resulting from increased net O₃ production. Large NO_x mixing ratios ~~arose at Dome C~~ arise from a combination of changes in continuous sun light, shallow mixing height and significant NO_x ~~snow emission flux~~ emissions by surface snow (F_{NO_x}). During 23 December 2011–12 January 2012 median F_{NO_x} was twice that during the same period in 2009–2010 due to significantly larger atmospheric turbulence and a slightly stronger snowpack source. A tripling of F_{NO_x} in December 2011 was largely due to changes in snow pack source strength caused primarily by changes in NO₃⁻ concentrations in the snow skin layer, and only to a secondary order by decrease of total column O₃ and associated increase in NO₃⁻ photolysis rates. ~~Systematic changes in~~ A source of uncertainty is the quantum yield of ~~photolysis over time~~ may contribute to the observed F_{NO_x} variability nitrate photolysis in natural snow, which may change over time as the snow ages.

1 Introduction

The nitrogen oxides NO and NO₂ (NO_x = NO + NO₂) play a key role in the polar troposphere in determining its oxidation capacity, defined here as the sum of O₃, HO_x radicals, and hydrogen peroxide (H₂O₂). The influence is achieved via photolysis of NO₂, the only source for in situ production of tropospheric O₃, through shifting HO_x radical partitioning towards the hydroxyl radical (OH) via the reaction NO + HO₂ → NO₂ + OH, and finally through reactions with peroxyradicals NO + HO₂ (or RO₂) which compete with the formation of peroxides (H₂O₂ and ROOH).

Atmospheric mixing ratios of NO_x in the atmospheric boundary layer of coastal Antarctica are small, with average NO_x values in summer not exceeding 30 pptv (Bauguitte et al., 2012). The build up of large mixing ratios is prevented by gas-phase formation of halogen nitrates (e.g. BrNO₃, INO₃) followed by their heterogeneous loss (Bauguitte et al., 2012). Conversely, mixing ratios of NO_x on the East Antarctic Plateau are unusually large, similar to those from the mid-latitudes (Davis et al., 2008; Slusher et al., 2010; Frey et al., 2013). Such large mixing ratios of NO_x were found to arise from a combination of several factors: continuous sunlight, location at the bottom of a large air drainage basin, low temperatures leading to low primary production rates of HO_x radicals, significant emissions of NO_x from surface snow, and a shallow boundary layer (Davis et al., 2008; Frey et al., 2013, and refs. therein).

Snow emissions of NO_x, observed at several polar locations (e.g. Jones et al., 2001; Honrath et al., 2000b), are driven by UV-photolysis of nitrate (NO₃⁻) in snow (Honrath et al., 2000b; Simpson et al., 2002) and are now considered to be an essential component of air-snow cycling of oxidised nitrogen species above the polar ice sheets (Davis et al., 2008; Frey et al., 2009b) and likely also above mid-latitude snow packs (Honrath et al., 2000a; Fisher et al., 2005). Atmospheric dynamics, i.e. vertical mixing strength and mixing height, can explain some of the observed temporal variability and site-specific chemical composition of the lower troposphere at South Pole and Summit, Greenland (~~?Neff et al., 2008~~) (Neff et al., 2008; Van Dam et al., 2013). Recently, the very strong diurnal cycle of mixing ratios of NO_x observed at Dome C, East Antarctic Plateau, during

summer was shown to result from the interplay between boundary layer mixing and emissions from the photochemical snow source; during calm periods a minimum of NO_x mixing ratios occurred around local noon and a maximum in the early evening coinciding with the development and collapse of a convective boundary layer (Frey et al., 2013). A key parameter of the physical atmospheric processes at play is the turbulent diffusivity of the atmosphere, which controls the mixing height, h_z , of the atmospheric boundary layer and contributes to the magnitude of the flux of trace chemical species emitted by the snow (e.g. Frey et al., 2013).

The impact of NO_x emissions from snow on the oxidation capacity of the lower troposphere in summer can be significant. For example, NO_x snow emissions can result in net ~~ozone~~- O_3 production as observed in the interior of Antarctica (Crawford et al., 2001; Legrand et al., 2009; Slusher et al., 2010) as well as unusually large mixing ratios of hydroxyl ~~radical levels~~ radicals as detected at South Pole (Davis et al., 2008, and refs. therein). Furthermore, in Antarctica the gas phase production of hydrogen peroxide (H_2O_2), the only major atmospheric oxidant preserved in ice cores, is sensitive to NO released by the surface snowpack (e.g. Frey et al., 2005, 2009a). A steady-state analysis of ratios of NO_2 : NO at Dome C suggested that mixing ratios of peroxy radicals (not measured at the time) are possibly larger at Dome C than any previous observations in air above polar snow (Frey et al., 2013).

The quantitative understanding of emissions of NO_x from snow remains incomplete, but it is a research priority to be able to parameterise global models to assess for example global impacts of chemical air-snow exchange on tropospheric ~~ozone~~- O_3 (e.g. Zatzko et al., 2013). Emissions of NO_x from snow at Dome C are among the largest observed above either polar ice sheet, but are typically underestimated by models, especially at large solar zenith angles (Frey et al., 2013). ~~One significant model uncertainty is the quantum yield of nitrate photolysis in snow, which is related to the location of the nitrate ion in snow grains, and needs to be better constrained by observations (Frey et al., 2013; Meusinger et al., 2014).~~

The study presented here was part of the comprehensive atmospheric chemistry campaign OPAL (Oxidant Production and its Export from Antarctic Lands) in East Antarctica (Preunkert et al., 2012) and provided the opportunity to measure NO_x mixing ratios and flux

during a second summer season, after a previous campaign in 2009–2010 (Frey et al., 2013). The study objectives were firstly to extend the existing data set with mixing ratio profiles of the lower atmosphere and the firn air (interstitial air) column of the upper snow pack. Secondly, to investigate if observed $\text{NO}_2:\text{NO}$ ratios are consistent with measurements of hydroxyl and halogen radicals. And thirdly, to analyse the main drivers of the atmospheric NO_x emission flux from snow.

2 Methods

The measurement campaign of 50 days took place at Dome C (75.1°S , 123.3°E , 3233 m) from 23 November 2011 to 12 January 2012. Similar to the 2009–2010 campaign atmospheric sampling was performed from an electrically heated lab shelter (Weatherhaven tent) located in the designated clean-air sector 0.7 km upwind (South) of Concordia station (~~see map in Frey et al., 2013~~) (Frey et al., 2013, Fig. 1a). All times are given as local time (LT), equivalent to UTC + 8 h, and during the study period the sun always remained above the horizon.

2.1 NO_x concentration ~~and flux~~ measurements and uncertainties

Three 20 m-long intake lines (Fluoroline 4200 high purity PFA, I.D. 4.0 mm) were ~~mounted on~~ attached to a mast ~~about~~ located at 15 m from the lab shelter into the prevailing wind to continuously sample air at 0.01, 1.00 and 4.00 m above the natural snow pack. The intake lines were away from the influence of the drifted snow around the lab shelter. On 9 January 2012 vertical profiles of the lower atmosphere were sampled by attaching a 100 m-long intake line to a helium-filled weather balloon, which was then manually raised and lowered. During selected time periods firn air was sampled, to depths 5–100 cm, by means of a custom built probe. The probe consisted of a tube (10 cm diameter) which was lowered vertically into a pre-cored hole to the chosen snow depth, passing through a disc (1 m diameter) resting on the snow surface. The disk had a lip of 10 cm protruding into the snow. The lip and

disk minimised preferential pumping of ambient air along the tube walls. The air intake was mounted ~~at the bottom end of the vertical tube~~ so that only air from the bottom and sides could enter, using small horizontal holes ~~, could enter~~ at 0-10 cm above the open bottom end of the vertical tube. All probe components were made from UV-transparent plastic (Plexiglas Sunactive GS 2458). Furthermore, 2×3 m sheets of UV-opaque (Acrylite OP-3) and UV-transparent (Acrylite OP-4) plexiglass, mounted on aluminium frames at 1 m above the snow surface, were used to deduce the effect of UV radiation on the mixing ratio of NO_x in the interstitial air and avoid at the same time any temperature effect altering the snow surface.

To measure NO_x the same 2-channel chemiluminescence detector (CLD) and experimental set up as during the 2009–2010 campaign were used ~~(instrument schematic in Frey et al., 2013)~~ (Frey et al., 2013, Fig.1b). Channel one of the CLD measured atmospheric mixing ratios of NO whereas the other channel determined the sum of the mixing ratios of NO and NO originating from the quantitative photolytic conversion of NO_2 . The difference between the two channels was used to calculate atmospheric mixing ratios of NO_2 . The three sample inlets were connected inside the lab shelter to a valve box, which automatically switched the CLD between sampling heights on a 90 s duty cycle. As described below, the 10-minute average concentration difference ΔNO_x between the 0.01 and 1.0 m inlets is used to estimate flux. Therefore, 10-minute mean ΔNO_x values are calculated on average from two sets of two subsequent 90 s intervals, separated by a 90 s interval during which the 4.0 m inlet was measured. Baseline count rates were determined by adding excess O_3 to sample air in a pre-chamber so that all electronically excited NO_2 has returned to ground state when reaching the reaction chamber. The baseline was measured for 60 s every 13.5 min alternating between all three inlets. The NO sensitivity of the CLDs was determined every 14 h by standard addition to the sample air matrix of a 1 ppm NO/NO_2 mixture (UK National Physics Laboratory traceable BOC certified), which is further diluted to 4 ppbv of NO. During standard runs also the conversion efficiency (CE) of the photolytic converter was determined by addition of a known mole fraction of NO_2 . This was achieved by gas phase titration of the NO/NO_2 mixture to NO_2 by O_3 generated

from a pen-ray lamp, and monitoring the un-titrated NO mole fraction. The instrument artefact originating from NO_x producing surface reactions in inlets and reaction cells was determined by overflowing the instrument inlet with scrubbed ambient air supplied by a pure air generator (Eco-Physics PAG003). The artefact was measured every 14 h, offset by 7 h to the calibration runs.

The CLD employed converts also mean wind direction during the measurement period was from S (176°) with an average speed of 4.0 ms⁻¹ (Fig. 1b). During 2.5% of the time winds came from the direction of Concordia station, i.e. the 355-15° sector (Frey et al., 2013, Fig.1a), potentially carrying polluted air from the station power generator to the measurement site. For example, during Period III, winds rotated 4 times through northerly directions (Fig. 1b). Pollution spikes in the raw 1-s data typically exceeded 10 ppbv of NO_x and were effectively removed before computing the 1-min averages by applying a moving 1-min standard deviation (σ) filter. Observations were rejected when 1- σ of NO and NO₂ mixing ratios within a 1-min window exceeded 24 and 90 pptv, respectively.

The CLD employed also converts nitrous acid (HONO) to NO in the photolytic converter and thus HONO sampled by the CLD is an interference, as discussed previously (Frey et al., 2013). Average mixing ratios of HONO at 1 m above the snowpack measured with the LOPAP (Long Path Absorption Photometer) technique were ~ 35 pptv (Legrand et al., 2014). The corresponding downward correction for NO₂ at 1 m above the snowpack is ~ 5%. However the LOPAP technique may overestimate the mixing ratio of HONO owing to an interference with by pernitric acid (HO₂NO₂) (Legrand et al., 2014). True corrections of NO₂ inferred from modelled HONO mixing ratios (Legrand et al., 2014) are more likely to be on the order of < 1.5%. Due to the uncertainty in absolute mixing ratios of HONO, no correction of NO_x values for the HONO interference was applied.

The presence of strong gradients in mixing ratios of inferred by Legrand et al. (2014) can potentially lead to an overestimate of concentration differences between 0.01 and 1.0 used below to derive the vertical flux. During the OPALE campaign the atmospheric life time of, τ_{NO_x} , ranged between 3(12:00LT) and 7(00:00LT), whereas that of, τ_{HONO} , ranged between 4.5(12:00LT) and 24(00:00LT) (Legrand et al., 2014). The life time of is comparable to

the typical transport times of ~ 10 between the surface and 1 at Dome C in summer (Frey et al., 2013). Hence, ratios as well as corresponding corrections required for are not constant with height above the snow surface. No gradients of mixing ratios were measured but modelled values were 18.8 and 10.2 at noon, and 15.3 and 12 at midnight, at 0.1 and 1.0, respectively (Legrand et al., 2014). Corresponding corrections of mean mixing ratios for are 1.3–1.5% with a maximum difference of 0.2% between 0.1 and 1.0. Thus, at Dome C a strong gradient in the mixing ratios of was a negligible effect on the mixing ratios of measured at 0.1 and 1.0 and thus a negligible effect on the estimated flux.

The thermal decomposition of HO_2NO_2 in the sample lines or photolytic converter of the CLD could also cause a positive bias of NO_x . Spike tests showed that the sample air residence time in the total volume of inlets and CLD is ~ 4 s (Frey et al., 2013). At a sample flow rate of $5.0 \text{ STP} - \text{L min}^{-1}$ the residence time in the combined volume of photolytic converter and CLD reaction cell is estimated to be < 2 s. Atmospheric lifetimes of $\tau_{\text{HNO}_4-\text{HO}_2\text{NO}_2}$, $\tau_{\text{HO}_2\text{NO}_2}$, with respect to thermal decomposition to $\text{HO}_2 + \text{NO}_2$ were calculated at mean ambient pressure (645 mb) using rate coefficients after Jacobson (1999). $\tau_{\text{HNO}_4-\text{HO}_2\text{NO}_2}$ decreases from 8.6 h at mean ambient temperature assumed in the sample intake lines (-30°C) to 7 s at the maximum observed temperature in the photolytic converter (30°C). Therefore, NO_2 production from HO_2NO_2 thermal decomposition is negligible in the sample intake lines, but approximately 25% of all HO_2NO_2 present may be converted to NO_2 in the photolytic converter. A recent airborne campaign above the East Antarctic Plateau showed mean summertime atmospheric mixing ratios of HO_2NO_2 between 0 and 50 m of 65 pptv with maxima about twice as large (Slusher et al., 2010). HO_2NO_2 present at these values could potentially produce 33–66–16–32 pptv of NO_2 in the photolytic converter equivalent to 16–328–16% of the average NO_2 mixing ratio measured at 1 m. We On 5 January 2012 we attempted to test for the presence of HO_2NO_2 by passing ambient air through a 50 m intake heated to 50°C before it entered the CLD. However, during the tests no significant change in NO_2 was detected.

The presence of strong gradients in mixing ratios of HONO inferred by Legrand et al. (2014) can potentially lead to an overestimate of the NO_x concentration

differences between 0.01 and 1.0 m used below to derive the vertical NO_x flux. During the OPAL campaign the atmospheric life time of NO_x , τ_{NO_x} , ranged between 3 h (12:00 LT) and 7 h (00:00 LT), whereas that of HONO, τ_{HONO} , ranged between 4.5 min (12:00 LT) and 24 min (00:00 LT) (Legrand et al., 2014). The life time of HONO is comparable to the typical transport times of ~ 10 min between the surface and 1 m at Dome C in summer (Frey et al., 2013). Hence, HONO : NO_x ratios as well as corresponding corrections required for NO_2 are not constant with height above the snow surface. No gradients of HONO mixing ratios were measured but modelled values were 18.8 and 10.2 pptv at noon, and 15.3 and 12 pptv at midnight, at 0.1 and 1.0 m, respectively (Legrand et al., 2014). Corresponding corrections of mean NO_2 mixing ratios for HONO are 1.3–1.5% with a maximum difference of 0.2% between 0.1 and 1.0 m. Thus, at Dome C a strong gradient in the mixing ratios of HONO was a negligible effect on the mixing ratios of NO_x measured at 0.1 and 1.0 m and thus a negligible effect on the estimated NO_x flux.

2.2 NO_x flux estimates

The turbulent flux of NO_x , F_{NO_x} , was estimated using the integrated flux gradient method (e.g. Lenschow, 1995) and mixing ratios of NO_x measured at 0.01 and 1.0 m. F_{NO_x} in the surface layer is parameterised according to the Monin–Obukhov similarity theory (MOST) whose predictions of flux-profile relationships at Halley, an Antarctic coastal site of the same latitude as Dome C , agree well with observations (Anderson and Neff, 2008, and references therein):

$$F_{\text{NO}_x} = -\frac{\kappa u_* z}{\Phi_h\left(\frac{z}{L}\right)} \frac{\partial c}{\partial z} \quad (1)$$

with the von Karman constant κ (set to 0.40), friction velocity u_* , measurement height z , concentration gradient $\partial c/\partial z$, and $\Phi_h\left(\frac{z}{L}\right)$ an empirically determined stability function for heat with L as the Monin–Obukhov length. Assuming constant flux across the layer between

the two measurement heights z_1 and z_2 allows the integration to be solved and yields:

$$F_{\text{NO}_x} = - \frac{\int_{z_1}^{z_2} \kappa u_* \partial c}{\int_{z_1}^{z_2} \Phi_h \left(\frac{z}{L} \right) \frac{\partial z}{z}} = - \frac{\kappa u_* [c(z_2) - c(z_1)]}{\int_{z_1}^{z_2} \Phi_h \left(\frac{z}{L} \right) \frac{\partial z}{z}} \quad (2)$$

Stability functions Φ_h used are given in Frey et al. (2013), while their integrated forms can be found in Jacobson (1999). Friction velocity u_* and L were computed from the three-dimensional wind components (u , v , w) and temperature measured at 25 Hz by a sonic anemometer (Metek USA-1) mounted next to the uppermost NO_x intake line, at 4 m above the snow surface. Processing of raw data in 10 min blocks included temperature cross-wind correction and a double coordinate rotation to force mean w to zero (Kaimal and Finnigan, 1994; Van Dijk et al., 2006). Equation (2) implies that a positive flux is in upward direction, equivalent to snow pack emissions and a negative flux is in downward direction, equivalent to deposition.

The application of MOST requires the following conditions to be met: (a) flux is constant between measurement heights z_1 and z_2 , (b) the lower inlet height z_1 is well above the aerodynamic roughness length of the surface, (c) the upper inlet height z_2 is within the surface layer, i.e. below 10% of the boundary layer height h_z (Stull, 1988), and (d) z_1 and z_2 are far enough apart to allow for detection of a significant concentration difference $[c(z_2) - c(z_1)]$. ~~During summer at Dome C conditions-~~

Condition (a) is met in the surface layer if the chemical lifetime τ_{chem} of NO_x is much longer than the turbulent transport time scale τ_{trans} . Based on observed OH and HO_2 the τ_{chem} for NO_x is estimated to be 3 h at 1200 LT and 7 h at 0000 LT during OPALE (Legrand et al., 2014). Estimating τ_{trans} following the approach described previously (Frey et al., 2013, Eq. 6 and 7) yields 0.6, 1.7 and (b) are 2.5 min during the day (0900-1700 LT), the typical time of BL collapse (1700-1900 LT) and during the night (1900-0900 LT), respectively. Thus, τ_{chem} exceeds τ_{trans} by at least a factor 100, confirming that vertical mixing always dominates over the gas phase photochemical sink and flux can be assumed constant between the two inlets. Condition (b) is met as discussed in Frey et al. (2013). For (c) the upper inlet height of 1 m is compared to estimates of mix-

ing height h_z from the MAR model (Gallée et al., 2015). The MAR model has been validated previously over the Antarctic Plateau, focusing on Dome C, during winter (Gallée and Gorodetskaya, 2010) and now also during summer (Gallée et al., 2015). Calculated flux values of NO_x were removed when $h_z < 10$ m resulting in the removal of 22 % (773 values) of all available 10 min flux averages. Flux estimates are removed specifically during the evening and night, when the BL is shallow. Hence, fluxes during night time are less well constrained, but nevertheless support a significant diurnal cycle (Frey et al., 2013, Fig. 6b,g and Fig. 9). For (d) 10 min averages of $[c(z_2) - c(z_1)]$ not significantly different from zero, i.e. smaller than their respective $1-\sigma$ standard error, were not included in the calculation of the flux of NO_x . The $1-\sigma$ standard error in $[c(z_2) - c(z_1)]$ was determined by error propagation of the $1-\sigma$ standard error of NO_x mixing ratios. A total of 8 % (303 values) of all available 10 min flux averages were not significantly different from zero and thus removed.

In summary, the restrictions imposed by MOST and NO_x measurement uncertainty justify placing inlets at 0.01 and 1.0 m and lead to the removal of 30 % (1076 values) of all available flux estimates. The total uncertainty of the 10 min NO_x flux values due to random error in $[c(z_2) - c(z_1)]$ (31 %), u_* (3 % after Bauguitte et al., 2012) and measurement height (error in $\ln(z_2/z_1)$ of $\sim 7\%$) amounts to 32 %.

2.3 MAX-DOAS observations

Scattered sunlight was observed by a ground-based UV-visible spectrometer, in order to retrieve bromine oxide (BrO) column amounts. The instrument was contained in a small temperature-controlled box, which was mounted onto a tripod at 1 m above the snow surface. An external gearbox and motor scanned the box in elevation (so-called Multiple Axis). Spectra were analysed by Differential Optical Absorption Spectroscopy (DOAS), the combination being known as the MAX-DOAS technique. See Roscoe et al. (2014) for more details of apparatus and analysis. Briefly, the observed spectrum contains Fraunhofer lines from the Sun's atmosphere, which interfere with absorption lines in the Earth's atmosphere and are removed by dividing by a reference spectrum. The amounts of absorbers in the Earth's

atmosphere are found by fitting laboratory cross-sections to the ratio of observed to reference spectra, after applying a high-pass filter in wavelength (the DOAS technique).

In our case the spectral fit was from 341 to 356 nm, and the interfering gases O₃, O₄ (oxygen dimer) and NO₂ were included with BrO. The analysis was done with two reference spectra, one from near the start of the campaign in December, the other following the addition of a snow excluder in January, necessary because it also contained a blue glass filter with very different spectral shape. The analysis was restricted to cloud-free days or part-days. In MAX-DOAS geometry, the stratospheric light path is almost identical in low-elevation and zenith views, so stratospheric absorption is removed by subtracting simultaneous zenith amounts from low-elevation slant amounts, important for BrO as there is much in the stratosphere.

To find the vertical amounts of BrO radicals the MAX-DOAS measurements were evaluated as follows: we divided by the ratio of the slant path length to the vertical (the Air Mass Factor, AMF), calculated by radiative transfer code (Mayer and Kylling, 2005), assuming all the BrO was in the lowest 200 m.

2.4 Ancillary measurements and data

Other co-located atmospheric measurements included mixing ratios of OH radicals and the sum of peroxy radicals (RO₂) at 3 m using chemical ionisation mass spectrometry (Kukui et al., 2014) and mixing ratios of O₃ at 1 m with a UV absorption monitor (Thermo Electron Corporation model 49I, Franklin, Massachusetts). Photolysis rate coefficients, J , were determined based on actinic flux, I , measured at ~ 3.50 m above the snow surface using a Met-Con 2π spectral radiometer equipped with a CCD detector and a spectral range from 285 to 700 nm (further details in Kukui et al., 2014). Total column O₃ above Dome C was taken from ground based SAOZ (Système d'Analyse par Observation Zenitale) observations (http://saoz.obs.uvsq.fr/SAOZ_consol_v2.html). Standard meteorology was available from an automatic weather station (AWS) at 0.5 km distance and included air temperature (Vaisala PT100 DTS12 at 1.6 m), relative humidity (at 1.6 m), wind speed and direction (Vaisala WAA 15A at 3.3 m). ~~Photolysis rate coefficients, J , were determined based on actinic flux, I , measured at ~ 3.50 above the snow surface with a Met-Con 2π spectral radiometer equipped~~

with a CCD detector and a spectral range from 285 to 700 (see also Kukui et al., 2014). The mixing height h_z of the atmospheric boundary layer was calculated from simulations with the MAR model as the height where the turbulent kinetic energy decreases below 5% of the value of the lowest layer of the model (Gallée et al., 2015).

5 During this study NO_3^- concentrations in snow were measured every 2–3 days in the surface skin layer, i.e. in the top 0.5 cm of the snowpack, as well as in shallow snow pits within the clean-air sector. Snow NO_3^- concentrations were determined using clean sampling procedures and a continuous flow analysis technique (e.g. Frey et al., 2009b). ~~Total column above Dome C was taken from ground-based SAOZ (Système d'Analyse par Observation Zenitale) observations ().~~ The mixing height h_z of the atmospheric boundary layer was calculated from simulations with the MAR model as the height where the turbulent kinetic energy decreases below ~~5% of the value of the lowest layer of the model (?). % based on replicate standard~~ measurements. Due to a systematic shift in the NO_3^- standard response in between individual batch runs due to a calibration issue (Berhanu et al., 2014) the accuracy is larger than usual. The overall accuracy including systematic errors in calibration and collection of just the top few mm of snow is of the order of 20%, and is therefore comparable to the spatial variability of NO_3^- in surface snow at Dome C (France et al., 2011). For the discussion below it should be borne in mind that temporal changes of NO_3^- concentrations observed in surface snow are >50% (Fig. 7b) and therefore significantly larger than the measurement accuracy.

2.5 Modelling NO_3^- photolysis

The flux of NO_2 , F_{NO_2} , from the snowpack owing to photolysis of the NO_3^- anion in the snowpack can be estimated as the depth-integrated photolysis rate of NO_3^-

$$25 \quad F_{\text{NO}_2} = \int_{z=0\text{m}}^{z=1\text{m}} [\text{NO}_3^-]_z J_z(\text{NO}_3^-) dz \quad (3)$$

where $J_z(\text{NO}_3^-)$ is the photolysis rate coefficient of reaction $\text{NO}_3^- + h\nu \rightarrow \text{NO}_2 + \text{O}^-$ at depth, z , in the snowpack. $[\text{NO}_3^-]_z$ is the amount of **nitrate-NO₃⁻** per unit volume of snow at depth, z , in the snowpack. $J(\text{NO}_3^-) - J_z(\text{NO}_3^-)$ is calculated as described in France et al. (2010) using a radiative transfer model, TUV-snow (Lee-Taylor and Madronich, 2002), to calculate irradiances within the snowpack as a function of depth. The optical properties and detailed description of the Dome C snowpack are reported in France et al. (2011). Values of depth-integrated flux were calculated as a function of solar zenith angle and scaled by values of $J(\text{NO}_3^-)$ measured by the Met-Con 2π spectral radiometer described above to account for changing sky conditions. Scaling by a measured value of $J(\text{NO}_3^-)$ is more accurate than previous efforts of scaling with a broad band UV instrument (e.g. France et al., 2011). The quantum yield and the absorption spectrum for **nitrate-NO₃⁻** photolysis in snow were taken from Chu and Anastasio (2003). For the discussion below it should be borne in mind that the calculated F_{NO_2} is a potential emission flux assuming that NO_2 is vented immediately after release from the snow grain to the air above the snow pack without undergoing any secondary reactions.

3 Results and discussion

3.1 NO_x observations in ambient and firn air

In summer 2011–2012 atmospheric mixing ratios of NO_x with strong diurnal variability were observed (Fig. 1c), similar to the 2009–2010 season, and showed maximum median levels in firn air of ~ 3837 pptv, which rapidly decreased to 319 pptv at 0.01 m and 213 pptv at 1.0 m (Table 1). As seen previously at Dome C and other locations, NO_x mixing ratios were weakly but significantly anti-correlated with wind speed (e.g. at 1.0 m $R^2 = 0.14$, $p < 0.001$) $R = -0.37$, $p < 0.001$, especially when only the time period of the daily collapse of the convective boundary layer, i.e. 1700–1900 LT, was considered ($R = -0.45$, $p < 0.001$), and their diurnal cycle was dampened during storms (Fig. 1b and cb-c).

The two main differences between summer 2011–2012 and summer 2009–2010 are a strong intra-seasonal ~~trend~~ variability and larger atmospheric mixing ratios. A significant increase of NO_x mixing ratios at 1.0 m from low values in ~~late November 2011~~ (Period I. (23–30 November 2011)) occurred in two steps: a small rise in ~~the first week of December~~ (Period II. (1–8 December 2011)), followed by a strong increase of daily averages from 300 to 1200 pptv during at the beginning of Period III. (9–11 December 2011) (Period III.) (Fig. 1c). After that NO_x mixing ratios gradually dropped over 10 days (~~Periods~~ Period III.–IV.) to ~~late November average concentrations of ~ 120~~ median concentrations of ~ 120 pptv, slightly lower than observed in late November (Fig. 1c, Table 2). During Period III. (9–22 December 2011) (Period III.) the median concentration of NO_x at 1.0 m was 451 pptv, about 2.5 times that during the same time period in 2009, but similar thereafter (Fig. 1c, Table 2).

The NO_x fluxes, F_{NO_x} , between 0.01 and 1.0 m were mostly emissions from the snow surface, with a median ~~(range)~~ of 1.6 ~~(0.4–2.9)~~ $\times 10^{13}$ molecule $\text{m}^{-2} \text{s}^{-1}$. Median values of F_{NO_x} at midnight and at noon were 0.4 and 2.9×10^{13} molecule $\text{m}^{-2} \text{s}^{-1}$, respectively (Table 1). During Period III. F_{NO_x} showed an increase by a factor 3, approximately around the same time when atmospheric mixing ratios of NO_x increased (Period III.) (Fig. 1d, Table 2). The median flux of NO_x during 9–22 December 2011 reached 3.1×10^{13} molecule $\text{m}^{-2} \text{s}^{-1}$, about almost 5 times the season median from 2009–2010. During 23 December to 12 January (Period IV.) the median flux of NO_x in 2011–2012 was about twice that observed in 2009–2010 (Table 2). Potential causes of significant variability in mixing ratios and flux on seasonal time scales are discussed in Sect. 3.5.

3.2 The lower atmosphere-firn air profile

On 9 January 2012 a total of 12 vertical atmospheric profiles of NO_x mixing ratios were measured between 11:30 and 23:30 LT. The lower 100 m of the atmosphere appear well mixed throughout the afternoon, with modelled mixing heights h_z of 200–550 m and observed turbulent diffusion coefficients of heat K_h of $\sim 0.1 \text{ m}^2 \text{ s}^{-1}$ (Fig. 2). However, in the late afternoon K_h values decreased gradually over a few hours to reach in the evening levels half those during the day thereby giving evidence of strongly reduced vertical mixing. Furthermore,

around 18:30 LT modelled h_z values decreased within minutes from 550 to < 15 m height (Fig. 2a) illustrating the collapse of the convective boundary layer typically observed at Dome C in the early evening during summer (King et al., 2006). At Dome C rapid cooling of the surface in the evening results in a strong shallow surface inversion (e.g. Frey et al., 2013), and is illustrated by a decrease in downward long-wave radiation and a negative heat flux, as observed in the evening of 9 January 2012 (Argentini et al., 2014, Fig.4). It follows that NO_x snow emissions are trapped near the surface and caused, which then leads to a significant increase in NO_x mixing ratios below 15 m height measured almost immediately after collapse of the boundary layer (Fig. 2). During 22:20–22:40 LT a small increase in K_h , due to the nightly increase in wind shear (see Frey et al., 2013), was sufficient to cause upward mixing of NO_x accumulated near the surface to ~ 35 m height (Fig. 2). The vertical balloon soundings further underline the unique geographical setting of Dome C or other sites of similar latitude on the East Antarctic Plateau where air chemistry is dominated by strong diurnal cycles, both in down-welling solar radiation and atmospheric stability, contrasting South Pole where diurnal changes are absent and changes are more due to synoptic variability (Neff et al., 2008).

A vertical profile of mixing ratios of NO_x and O_3 in firn air was measured on 12 January 2012 between 10:00 and 18:00 LT, for which depths were sampled in random order for 30–60 min each. Mixing ratio maxima of NO and NO_2 were ~ 1 and 4 ppbv, respectively, about one order of magnitude above ambient air levels (Table 1), and occurred at 10–15 cm depth, slightly below the typical e-folding depth of 10 cm of wind pack snow at Dome C (France et al., 2011) (Fig. 3a). NO dropped off quickly with depth, reaching 55 pptv at 85 cm, whereas NO_2 decreased asymptotically approaching ~ 2 ppbv (Fig. 3a). NO_3^- concentrations in snow under the firn air probe did not follow the exponential decrease with depth typically observed at Dome C (e.g. Erbland et al., 2013), ~~but~~. The firn air probe was installed onto untouched snow, and only removed after the end of the atmospheric sampling period. Thus contamination due to local activity appears unlikely, but a local anomaly remains a possibility as snow pits 5 m next to the lab shelter showed a similar increase of concentration with depth (data not shown). But NO_3^- values within one e-folding depth were still in the

range measured further away (Profiles P1–P3 in Fig. 3a), justifying a discussion of vertical ~~trends–profiles of mixing ratios.~~

O₃ mixing ratios in firn air were always below ambient air levels, suggesting the snow pack to be an O₃ sink as observed previously for the snowpack on the Greenland ice sheet (Peterson and Honrath, 2001), and showed a significant anti-correlation with NO₂ (~~$R^2 = 0.7$~~ $R = -0.84$, $p < 0.001$). This is further evidence for significant release of NO_x by the snow matrix into the interstitial air, which then titrates O₃ through the reaction NO + O₃ → NO₂ + O₂ (Fig. 3). In particular, the ~~elevated concentration drop of O₃ mixing ratios by >10 ppbv at 45 cm depth~~ was not an outlier, ~~as indicated by the collocated drop of by >10 since collocated NO₂ mixing ratios were also significantly elevated~~ compared to adjacent snow layers, ~~but was possibly due to snow with large concentrations~~ (Fig. 3a). ~~However, no snow NO₃⁻ measurements were available to further investigate the origin of the NO₂ peak.~~ The observed vertical trends in NO_x suggest that below a few e-folding depths the open pore space of the upper snowpack holds a significant reservoir of NO₂ produced photochemically above, as hypothesized previously (Frey et al., 2013). In contrast, NO disappears at depths devoid of UV irradiance as it reacts with O₃.

3.3 Response to UV irradiance

Changes in surface downwelling UV irradiance lead to a quick response of mixing ratios and speciation of NO_x in ambient and firn air as observed during a partial solar eclipse and during a shading experiment (Fig. 4). The solar eclipse occurred early in the season, on 25 November 2011, and caused a decrease in ambient NO mixing ratios at 1.0 m by about 10 pptv or 10%, whereas NO₂ mixing ratios did not change significantly (Fig. 4a and b). The NO gas phase source, UV photolysis of NO₂, is reduced during the solar eclipse. But the sink of NO, the fast titration with O₃, is unaffected by the reduction in UV irradiance. During the shading experiment on 11 January 2012 plastic sheets were placed at 1 m above the snow surface, alternating in 30 min intervals between UV-opaque and UV-transparent materials. The impact of blocking incident UV irradiance (wavelengths < 380 nm) on firn air mixing ratios at 10 cm snow depth was up to 300 pptv or 30% decrease in mixing ratios

of NO, whereas mixing ratios of NO₂ increased at the same time by ~150 pptv or 5%, although often not statistically significant (Fig. 4c and d). Similar to the solar eclipse, the behavior of NO_x mixing ratios in firn air is in accordance with a disruption of the fast gas phase interconversion of NO_x species. Decrease of NO and increase of NO₂ mixing ratios are consistent with the suppression of NO₂ photolysis, which is both a NO source and a NO₂ sink.

Most importantly varying incident UV irradiance in the wavelength region of NO₃⁻ absorption (action spectrum maximum at 320 nm) over half-hourly time scales does not cause a depletion of NO₂ in firn air even though NO₂ is the main product of NO₃⁻ photolysis in the snowpack. A dampened UV response of NO₂ mixing ratios suggests that the NO_x reservoir present in the open pore space of the upper snow pack discussed above must be large as it is not depleted during 30 min filter changes at the sample pump rates used. One implication is that the impact of changes in incident UV irradiance on the snow source and thus NO_x flux and mixing ratios is only observable on diurnal and seasonal time scales.

3.4 NO₂:NO ratios, peroxy and halogen radicals

In 2011–2012 the NO₂:NO ratios at 1.0 m were up to 3 times larger than in 2009–2010 (Table 2). A previous steady-state analysis indicated that high peroxy and possibly halogen radical levels must be present to explain large deviations from the simple Leighton steady-state (Frey et al., 2013). During summer 2011–2012 median concentrations of RO₂ radicals at 3 m, thought to consist mainly of HO₂ and CH₃O₂, were 9.9×10^7 molecule cm⁻³ (Kukui et al., 2014). ~~To find the vertical amounts of radicals the MAX-DOAS measurements were evaluated as follows: we divided by the ratio of the slant path length to the vertical (the Air Mass Factor, AMF), calculated by radiative transfer code (Mayer and Kylling, 2005), assuming all the was in the lowest 200.~~

Figure 5 shows the BrO results, where the apparent vertical amounts at 15° are much larger than those at lower elevations – the AMFs are incorrect, and interestingly, as at Halley in 2007 (Roscoe et al., 2014), much of the BrO must be in the free troposphere. The average of BrO at the three elevations is about 0.8×10^{13} molecule cm⁻², with a slight decrease

during the campaign. The average at Halley in 2007 was about 2.5×10^{13} molecule cm^{-2} , so mixing ratios of BrO at Dome C are about a third those at Halley. The Dome C data were not inverted to determine the mixing ratio near the surface, but the changes in slant column with elevation angle are similar to those at Halley in 2007 (Roscoe et al., 2014). So if the Halley inversion results are simply divided by 3 the Dome C values imply 2 to 3 pptv of BrO near the surface.

~~The same~~ Assuming steady-state the total radical concentration $[\text{OX}] = [\text{HO}_2] + [\text{RO}_2] + 2[\text{XO}]$, with $\text{XO} = \text{BrO}, \text{ClO}$, can be calculated based on observed $\text{NO}_2 : \text{NO}$ ratios and $J(\text{NO}_2)$ (Ridley et al., 2000). Repeating the calculation as described by Frey et al. (2013) was repeated for austral summer 2011–2012 and yields an average of 2.6 in Frey et al. (2013) for 19 December 2011 to 9 January 2012 yields a median $[\text{OX}]$ of 2.2×10^9 molecule cm^{-3} or 134116 pptv of total radical concentrations (Ridley et al., 2000). The steady-state estimates of Median $[\text{RO}_2]$ radicals are therefore ~ 20 times those observed at mid-day by Kukui et al. (2014). While observed and radicals are too low to explain the large $[\text{HO}_2]$ of 9.9×10^7 molecule cm^{-3} or 5 ratios it is possible that at least part of this pptv observed during the same period (Kukui et al., 2014) and 3 pptv of BrO yield $[\text{OX}]$ of 11 pptv. Hence, the estimated total radical concentration exceeds observations by a factor 10.3. To estimate the impact of a potential interference by HO_2NO_2 we corrected the NO_2 mixing ratios, assuming that additional NO_2 is measured in the CLD from HO_2NO_2 thermal decomposition, equivalent to 25% (100%) of ambient HO_2NO_2 on the order of 130 pptv. We then find that the median steady-state estimate of total oxidant concentrations is still a factor 9.6 (3.3) larger than that observed. Thus, only a part of the inconsistency may be due to overestimated from a potential interference with explained by the interference with HO_2NO_2 (not measured) as discussed above.

3.5 Drivers of seasonal NO_x variability

On diurnal time scales NO_x mixing ratios at Dome C are controlled by the interplay between snow-pack snowpack source strength and atmospheric physical properties, i.e. turbulent diffusion coefficient of heat K_h of heat K_h and mixing height h_z of the boundary

layer (Frey et al., 2013). Indeed, ~~The~~ median diurnal cycles of NO_x mixing ratios during 1–8 December 2011 (in 2011–12 show with the exception of Period II.) ~~showed previously described behavior (Frey et al., 2013) with a strong maximum during 18:00–20:00 (1–8 December) previously described behaviour (Frey et al., 2013), that is a strong increase around 1800 LT and a minimum at 01:00LT, then during to maximum values, which last into the night time hours (Fig. 6a). Night-time peaks of NO_x are plausible if the weakening of snow emissions is offset by a corresponding decrease of the chemical sink of NO_x , i.e. the $\text{NO}_2 + \text{OH}$ reaction, assuming no significant change in h_z . This is consistent to a first order taking into account that observed OH concentrations (Kukui et al., 2014) and F_{NO_x} vary in a similar way, by up to a factor 5 between local noon and midnight.~~

During Period III. (9–22 December 2011 (Period III.) ~~at similar~~), noon time values ~~further increase of the primary maximum and generally large mixing ratios are similar to Period II. but the increase in the evening has a larger amplitude and generally larger mixing ratios prevail during night time (Fig. 6a).~~ During 23 December 2011–2012 January 2012 (Period IV.) ~~the diurnal cycle of increased NO_x mixing ratios returned to low values and small diurnal amplitudes (Fig. 6a). As expected the during Period III. are consistent with the observed NO_x emission flux F_{NO_x} between 0.01 and 1.0, which always peaked at local noon, but showed during 9–22 December 2011 (also showed during Period III.) a strong increase at all times of the day with a near doubling of the noon time median (Fig. 6b).~~ During Period IV. (23 December 2011–2012 January 2012) ~~the diurnal cycles of both NO_x mixing ratios and F_{NO_x} returned to low values and small diurnal amplitudes (Fig. 6a–b).~~

Below we evaluate potential causes of the unusual variability in NO_x mixing ratios and flux observed on seasonal time scales.

3.5.1 Atmospheric mixing vs. snow source strength

Similar to explaining diurnal NO_x cycles at Dome C the seasonal ~~trends variability~~ of daily mean NO_x mixing ratios during the first half of December 2011 can be attributed to a combination of changes in F_{NO_x} and h_z (Fig. 1). The strong increase of NO_x around 11 December 2011 falls into a ~~period~~ Period when F_{NO_x} almost tripled, ~~but while wind speeds~~

slightly decreased and shallow boundary layer depths prevailed with daily h_z maxima below 100–200 heights prevailed (Fig. 1). After, Table 2). For example, on 12 December and 13 December the modelled diurnal ranges of h_z were 3.4–224 m and 3.6–251 m, respectively, while sodar observations yielded 10–150 m and 5–125 m, respectively (Gallée et al., 2015). After 13 December 2011 F_{NO_x} remained at high values, thus, the decrease of NO_x mixing ratios appears to be primarily caused by daily maximum stronger upward mixing into a larger volume, i.e. wind speeds increased and daily h_z increasing to > 600 maxima grew, exceeding 600 m on 18 December 2011 (Fig. 1). After 23 December NO_x mixing ratios drop to low levels, due to smaller F_{NO_x} and a deep boundary layer (Fig. 1).

Trends in F_{NO_x} are controlled by variability in depends on atmospheric turbulence (K_h) and concentration differences difference (ΔNO_x), which in turn are is determined by the strength of the photolytic snow pack source at a given K_h (Eq. 21–2). However, the relative importance of K_h and snow pack source strength can vary. For example, during Period IV. (23 December 2011–12 January 2012 (Period IV.)) the median F_{NO_x} was 1.3×10^{13} molecule $\text{m}^{-2} \text{s}^{-1}$, about twice that observed during the same period in 2009–2010 (Fig. 6g; Table 2). The inter-seasonal difference can be explained by both, significantly larger atmospheric turbulence and more negative ΔNO_x during all times of the day in 2011–2012 (Fig. 6h and i). Median K_h was $0.08 \text{ m}^2 \text{ s}^{-1}$, double that in 2009–2010, and median ΔNO_x was -51 pptv compared to -32 pptv in 2009–2010 (Table 2).

In contrast, during 2011–2012 the observed intra-seasonal variability of F_{NO_x} is dominated by changes in the snow pack source strength. During Period III. (9–22 December 2011 (Period III.)) median K_h values ($\sim 0.05 \text{ m}^2 \text{ s}^{-1}$) and diurnal cycles were smaller than thereafter (Fig. 6c; Table 2), while ΔNO_x values were among the largest observed so far at Dome C, about three times those during the rest of the season, and therefore primarily caused the tripling of F_{NO_x} (Fig. 6d and i). In section 3.5.2 we'll discuss underlying causes of changes in the strength of the snow source.

Previously, non-linear HO_x - NO_x chemistry and the associated increase in NO_x lifetime were suggested to be an additional factor needed to explain large increases in NO_x mixing ratios observed at South Pole (Davis et al., 2008, and references therein). In order to assess

the relevance of this factor at Dome C we apply a simple box model to estimate net NO_x production rates as done previously (Frey et al., 2013). It is assumed that mixing is uniform and instantaneous, that the snow emission flux F_{NO_x} is the main NO_x source and the reaction with the OH radical is the dominant NO_x sink and

$$\frac{d[\text{NO}_x]}{dt} \sim \frac{F_{\text{NO}_x}}{h_z} - k[\text{NO}_2][\text{OH}] \quad (4)$$

where k is the respective reaction rate coefficient. In 2009–10 no OH observations were available at Dome C and average values from South Pole were used instead. In 2009–10 estimated net production rates of NO_x at night were on the order of 100 pptv h^{-1} and therefore explained the average increase in NO_x from 110 to 300 pptv observed from 1700 to 1900 LT (Frey et al., 2013). In 2011–12 the same analysis is repeated using OH measurements available for most of Period IV. (Kukui et al., 2014) as well as h_z calculated with the MAR model (Gallée et al., 2015). Resulting night time values of net NO_x production rates are with about 40 pptv h^{-1} smaller than in 2009–10 but again to a first order consistent with a smaller observed increase in NO_x mixing ratios in the evening hours; i.e. during Period IV. median NO_x increased between 1630 and 1930 LT from 114 to 242 pptv ((Fig. 6a,f). The above model is oversimplified as the very likely presence of HO_2NO_2 will modulate the diurnal variability of NO_x sinks and sources with an impact on NO_x lifetime as suggested by Davis et al. (2008). However without any information on the diurnal cycle of HO_2NO_2 at Dome C further modelling is not warranted.

3.5.2 Snow source strength

The NO_x flux observed above polar snow is on the order of 10^{12} to 10^{13} molecule $\text{m}^{-2} \text{s}^{-1}$ and contributes significantly to the NO_x budget in the polar boundary layer. At the lower end of the range are F_{NO_x} observations at Summit, Greenland (Honrath et al., 2002) and at Neumayer in coastal Antarctica (Jones et al., 2001) with 2.5×10^{12} molecule $\text{m}^{-2} \text{s}^{-1}$, whereas on the Antarctic Plateau F_{NO_x} values are up to ten times larger. For example, the

average F_{NO_x} at South Pole during 26-30 November 2000 was 3.9×10^{12} molecule $\text{m}^{-2} \text{s}^{-1}$ (Oncley et al., 2004), whereas at Dome C observed fluxes are 2-6 times larger, with seasonal averages of $8\text{-}25 \times 10^{12}$ molecule $\text{m}^{-2} \text{s}^{-1}$ (Frey et al., 2013, this work). Due to the uncertainties in the processes leading to NO_x production it had been difficult to explain inter-site differences, e.g. by simply scaling F_{NO_x} with UV irradiance and NO_3^- in the surface snow pack (Davis et al., 2004). Some of the variability in flux values may be due to differences in experimental set up or in the employed flux estimation method (e.g. Davis et al., 2004; Frey et al., 2013). For example, the F_{NO_x} estimates for South Pole are based on measured NO gradients only, inferring NO_x from photochemical equilibrium and using the Bowen ratio method (Oncley et al., 2004), whereas the F_{NO_x} estimates for Dome C are based on observations of both atmospheric nitrogen oxides (NO and NO_2) and the flux-gradient method (Frey et al., 2013).

Model predictions of F_{NO_x} show in general a low bias on the Antarctic Plateau when compared to observations. A first 3-D model study for Antarctica included NO_x snow emissions parameterised as a function of temperature and wind speed to match the observed F_{NO_x} at South Pole (Wang et al., 2007). However, the model under-predicts NO mixing ratios observed above the wider Antarctic Plateau highlighting that the model lacks detail regarding the processes driving the emission flux (Wang et al., 2007). The first model study to calculate F_{NO_x} based on NO_3^- photolysis in snow, as described in this work, reports $1\text{-}1.5 \times 10^{12}$ molecule $\text{m}^{-2} \text{s}^{-1}$ for South Pole in summer (Wolff et al., 2002), about a factor 4 smaller than the observations by Oncley et al. (2004) and up to 16 times smaller than what is needed to explain rapid increases in NO_x mixing ratios over a few hours (Davis et al., 2008, and references therein). Recent model improvements reduced the mismatch with the South Pole flux observations and included the use of updated absorption cross sections and quantum yield of the NO_3^- ion, as well as e-folding depths measured in surface snow on the Antarctic Plateau, and resulted in a factor 3 increase of flux calculated for South Pole (France et al., 2011). In light of major remaining uncertainties, which include the spatial variability of NO_3^- in snow and the quantum yield of NO_3^- photolysis (Frey et al., 2013), we discuss below the variability of F_{NO_x} observed at Dome C.

A number of factors may contribute to changes in snow source strength of NO_x . One possibility to explain increases in F_{NO_x} is that the NO_2 reservoir in the open pore space of the upper snowpack discussed above may undergo venting upon changes in atmospheric pressure. However, no statistically significant relationship between F_{NO_x} and atmospheric pressure is found (data not shown). The main cause of large F_{NO_x} values appears rather to be related to changes in snow production rates of NO_x from NO_3^- photolysis, which depend on the NO_3^- photolysis rate coefficient $J_{\text{NO}_3^-}$ and the NO_3^- concentration in the photic zone of the snow pack (Eq. 3).

Trends in down-welling UV irradiance due to stratospheric O_3 depletion were suggested previously to drive $J_{\text{NO}_3^-}$ and therefore F_{NO_x} and the associated increase in net production of surface O_3 observed at South Pole in summer since the 1990's (Jones and Wolff, 2003). At Dome C the observed increase in F_{NO_x} and strongly negative ΔNO_x values coincided with a period when total column O_3 declined from > 300 to about 250 DU (Fig. 7a and c). During Period III. (9–22 December 2011(Period III-)) the median column O_3 was about 8% lower than during the time periods before and after (Table 2). However, associated changes in $J_{\text{NO}_3^-}$ on the order of $\sim 10\%$ are too small to account alone for the observed tripling in F_{NO_x} (Fig. 6e; Table 2).

Instead changes in F_{NO_x} can be linked to the temporal variability of NO_3^- present in the snow skin layer. During ~~time periods~~ the end of Period II. and beginning of Period III. skin layer NO_3^- concentrations were up to two times larger than before and after ~~, coinciding with increased F_{NO_x}~~ (Fig. 7b and ~~c~~). F_{NO_x} is high during the end of Period II. and beginning of Period III. however drops off one week after the decrease of nitrate concentrations in surface snow (Fig. 7c). To confirm ~~this~~ the link between NO_x emissions and NO_3^- in snow F_{NO_2} values were modelled (Eq. 3) based on observed $J_{\text{NO}_3^-}$, daily sampling of skin layer NO_3^- and two depth profiles, at 100 m (P1) and 5 km (P2) distance from the lab shelter, in order to account for spatial and temporal variability ~~in~~ of NO_3^- concentrations of surface in snow. Modelled F_{NO_2} capture some of the temporal trends in observational estimates of F_{NO_x} confirming the link with $J_{\text{NO}_3^-}$ and NO_3^- concentrations (Fig. 7c). However, median

ratios of observed F_{NO_x} and modelled F_{NO_2} values are 30–50 during Period III. and 15–30 during Period IV. (Fig. 7c).

Disagreement between model and observations was previously attributed to uncertainties in the quantum yield of NO_3^- photolysis in natural snow (Frey et al., 2013). The model employed here uses a constant quantum yield, i.e. its value at the mean ambient temperature at Dome C (-30°C) of 0.0019 (Chu and Anastasio, 2003). ~~The~~ However, quantum yield may vary with time, as the same lab study reports a positive relationship between quantum yield and temperature (Chu and Anastasio, 2003). Comparison of time periods before and after 18 December 2011 shows an increase of mean air temperature from -34.2°C to -27.7°C and a decrease of its mean diurnal amplitude from 13 to 9.7 K (Fig. 1a). However, observations of F_{NO_x} showed behaviour opposite to that expected from a temperature driven quantum yield, i.e. F_{NO_x} values decreased as air temperature increased (Fig. 1a and d). Yet, the large diurnal amplitude of air temperature at Dome C could explain diurnal changes of F_{NO_x} by a factor 1.5–1.75. The temperature effect is however small when compared to the ~~observed~~ up to 20-fold change between night and day in F_{NO_x} , which ~~are-is~~ are driven by actinic flux. A recent lab study found that the quantum yield of photolytic loss of ~~nitrate-~~ NO_3^- from snow samples collected at Dome C decreased from 0.44 to 0.003 within what corresponds to a few days of UV exposure in Antarctica (Meusinger et al., 2014). The authors argue that the observed decrease in quantum yield is due to ~~nitrate-~~ NO_3^- being made of a photo-labile and a ~~photo-stabile~~ photo-stable fraction, confirming a previous hypothesis that the range of quantum yields reflects the location of NO_3^- within the snow grain and therefore availability to photolysis (~~Frey et al., 2013~~) (Davis et al., 2008; Frey et al., 2013). Thus, ~~observed-the~~ F_{NO_x} values observed at Dome C fall well within the range of predictions based on quantum yield values measured in Dome C snow snow samples from the same site, which exceed that used in the current model by a factor 2–200. A systematic decrease in quantum yield due to depletion of photo-labile NO_3^- in surface snow may have contributed to the observed decrease in F_{NO_x} after 22 December 2011. However, a lack of information on snow grain morphology or NO_3^- location within the snow grain limits further exploration of the impact of a time variable quantum yield on F_{NO_x} . It should be noted that during 2009–2010 large

skin layer NO_3^- values did not result in F_{NO_x} values comparable to those in 2011–2012 which may be due to a different partitioning between ~~photolabile and photostabile~~ photo-labile and photo-stable NO_3^- in surface snow (Fig. 7b and c; Table 2).

The consequences of large NO_x fluxes consist not only in contributing to high NO_x mixing ratios but also in influencing local O_3 production, as suggested by significantly higher surface O_3 mixing ratios (> 30 ppbv) during 9–22 December in 2011–2012 (Period III.) ~~than~~ compared to 25 ppbv in 2009–2010 (Fig. 7d).

4 Conclusions

Measurements of NO_x mixing ratios and flux carried out as part of the OPALE campaign at Dome C in 2011–2012 allowed to extend the existing data set from a previous campaign in 2009–2010.

Vertical profiles of the lower 100 m of the atmosphere confirm that at Dome C ~~strong diurnal cycles, both in down-welling solar radiation and atmospheric stability,~~ large diurnal cycles in solar irradiance and a sudden collapse of the atmospheric boundary layer in the early evening control the variability of NO_x mixing ratios and flux. In contrast, at South Pole diurnal cycles are absent and changes more due to synoptic variability (Neff et al., 2008). Large mixing ratios of NO_x at Dome C arise from a combination of several factors: continuous sunlight, large NO_x emissions from surface snow and shallow mixing depths after the evening collapse of the convective boundary layer. Unlike at South Pole it is not necessary to invoke non-linear HO_x - NO_x chemistry to explain increases in NO_x mixing ratios. However, uncertainties remain regarding atmospheric levels of HO_2NO_2 and its impact on NO_x life time being a temporary NO_x reservoir. Understanding atmospheric composition and air-snow interactions in inner Antarctica requires studies at both sites as they together encompass the spectrum of diurnal variability expected across the East Antarctic Plateau (King et al., 2006; Frey et al., 2013).

Firn air profiles suggest that the upper snow pack at Dome C is ~~a~~ an O_3 sink and holds below a few e-folding depths a significant reservoir of NO_2 produced photolytically above,

whereas NO disappears at depths devoid of UV as it reacts with O₃. Shading experiments showed that the presence of such a NO₂ reservoir dampens the response of NO_x mixing ratios above or within the snowpack due to changes in down-welling UV irradiance on hourly time scales. Thus, systematic changes in NO_x mixing ratios and flux due to the impact of UV on the snow source are only observable on diurnal and seasonal time scales.

First-time observations of BrO at Dome C suggest 2–3 pptv near the ground, with higher levels in the free troposphere similar to Halley, possibly originating from a sea ice source in coastal Antarctica (Theys et al., 2011) or from stratospheric descent (Salawitch et al., 2010). Assuming steady-state observed mixing ratios of BrO and RO₂ radicals are about a factor ten too low to explain the ~~large~~ NO₂:NO ratios found-measured in ambient air. ~~It is possible that~~ ~~-,likely-present-~~ The likely presence of HO₂NO₂ at Dome C ~~but-not-measured~~ during OPALÉ, (not measured) may cause an overestimate of NO₂ with the detection method employed and ~~may therefore explain~~ explain a part of this inconsistency.

During 2011–2012 NO_x mixing ratios and flux were larger than in 2009–2010 consistent with also larger surface O₃ mixing ratios resulting from increased net O₃ production. Large NO_x mixing ratios and significant variability during December 2011 were attributed to a combination of changes in mixing height and NO_x snow emission flux F_{NO_x} . Trends in F_{NO_x} were found to be controlled by atmospheric turbulence and the strength of the photolytic snowpack source, of which the relative importance may vary in time. Larger median F_{NO_x} values in 2011–2012 than those during the same period in 2009–2010 can be explained by both, significantly larger atmospheric turbulence and a slightly stronger snowpack source. However, the tripling of F_{NO_x} in December 2011 was largely due to changes in snow pack source strength driven primarily by changes in NO₃⁻ concentrations in the snow skin layer, and only to a secondary order by decrease of total column O₃ and associated increase in NO₃⁻ photolysis rates. Median ratios of observed F_{NO_x} and modelled F_{NO_2} values ranged from 15 to 50 using the quantum yield of NO₃⁻ photolysis reported by Chu and Anastasio (2003). Model predictions based on quantum yield values measured in a recent lab study on Dome C snow samples (Meusinger et al., 2014) yield 2–200 fold larger F_{NO_2} values encompassing observed F_{NO_x} . In particular, a decrease in quantum yield due to depletion of photo-labile NO₃⁻ in sur-

face snow may have contributed to the observed decrease in F_{NO_x} after 22 December 2011. Yet in 2009–2010 large skin layer NO_3^- values did not result in elevated F_{NO_x} values as seen in 2011–2012 possibly due to different partitioning of NO_3^- between a photo-labile and ~~photo-stabile fraction.~~ photo-stable fraction.

5 In summary the seasonal variability of NO_x snow emissions important to understand atmospheric composition above the East Antarctic Plateau depends not only on atmospheric mixing but also critically on ~~snow- NO_3^- concentrations and~~ concentration and availability to
10 photolysis in surface snow, as well as incident UV irradiance. Future studies ~~need to address~~ on the Antarctic Plateau need to reduce uncertainties in NO_2 measurements, obtain also
observations of HO_2NO_2 and assess how quantum yield of NO_3^- photolysis ~~varies in time in~~ snow varies
15 as a function of snow chemical and physical properties ~~thereby obtaining a more detailed view on the dynamics in the vertical redistribution of across the sunlit snowpack driven by photolysis and redeposition (e.g. Frey et al., 2009b).~~ This is important to be able
to close the mass budget of reactive nitrogen species between atmosphere and snow above
Antarctica.

Acknowledgements. M. M. Frey is funded by the Natural Environment Research Council through the British Antarctic Survey Polar Science for Planet Earth Programme. This study was supported by core funding from NERC to BAS's Chemistry & Past Climate Program. The OPAL project was funded by the ANR (Agence National de Recherche) contract ANR-09-BLAN-0226. National financial support
20 and field logistic supplies for the summer campaign were provided by Institut Polaire Français-Paul Emile Victor (IPEV) within programs No. 414, 903, and 1011. J. L. France and M. D. King wish to thank NERC NE/F0004796/1 and NE/F010788, NERC FSF 20 grants 555.0608 and 584.0609. We thank B. Jourdain for assistance with balloon soundings and firn air experiments, PNRA for meteorological data and IPEV for logistic support. We are also grateful to J. Dibb and D. Perovich
25 for valuable input on the design of the firn air probe. Collected data are accessible through NERC's Polar Data Centre.

References

Anderson, P. S. and Neff, W. D.: Boundary layer physics over snow and ice, *Atmos. Chem. Phys.*, 8, 3563–3582, doi:10.5194/acp-8-3563-2008, 2008.

Argentini, S., Petenko, I., Viola, A., Mastrantonio, G., Pietroni, I., Casasanta, G., Aristidi, E., and Genthon, C.: The surface layer observed by a high-resolution sodar at DOME C, Antarctica, *Annals of Geophysics*, 56, 1–10, doi:10.4401/ag-6347, 2014.

Bauguitte, S. J.-B., Bloss, W. J., Evans, M. J., Salmon, R. A., Anderson, P. S., Jones, A. E., Lee, J. D., Saiz-Lopez, A., Roscoe, H. K., Wolff, E. W., and Plane, J. M. C.: Summertime NO_x measurements during the CHABLIS campaign: can source and sink estimates unravel observed diurnal cycles?, *Atmos. Chem. Phys.*, 12, 989–1002, doi:10.5194/acp-12-989-2012, 2012.

Berhanu, T. A., Savarino, J., Erbland, J., Vicars, W. C., Preunkert, S., Martins, J. F., and Johnson, M. S.: Isotopic effects of nitrate photochemistry in snow: a field study at Dome C, Antarctica, *Atmos. Chem. Phys. Disc.*, 14, 33 045–33 088, doi:10.5194/acpd-14-33045-2014, 2014.

Chu, L. and Anastasio, C.: Quantum yields of hydroxyl radical and nitrogen dioxide from the photolysis of nitrate on ice, *J. Phys. Chem. A*, 107, 9594–9602, 2003.

Cohen, L., Helmig, D., Neff, W. D., Grachev, A. A., and Fairall, C. W.: Boundary layer dynamics and its influence on atmospheric chemistry at Summit, Greenland, *Atmos. Environ.*, 41, 5044–5060, doi:10.1016/j.atmosenv.2007.07.039, 2007.

Crawford, J. H., Davis, D. D., Chen, G., Buhr, M., Oltmans, S., Weller, R., Mauldin, L., Eisele, F., Shetter, R., Lefer, B., Arimoto, R., and Hogan, A.: Evidence for photochemical production of ozone at the South Pole surface, *Geophys. Res. Lett.*, 28, 3641–3644, 2001.

Davis, D. D., Seelig, J., Huey, G., Crawford, J., Chen, G., Wang, Y. H., Buhr, M., Helmig, D., Neff, W., Blake, D., Arimoto, R., and Eisele, F.: A reassessment of Antarctic plateau reactive nitrogen based on ANTCI 2003 airborne and ground based measurements, *Atmos. Environ.*, 42, 2831–2848, doi:10.1016/j.atmosenv.2007.07.039, 2008.

Davis, D. D., Chen, G., Buhr, M., Crawford, J., Lenschow, D., Lefer, B., Shetter, R., Eisele, F., Mauldin, L., and Hogan, A.: South Pole NO_x chemistry : an assessment of factors controlling variability and absolute levels, *Atmos. Environ.*, 38(32), 5275–5388, doi:10.1016/j.atmosenv.2004.04.039, 2004.

Erbland, J., Vicars, W. C., Savarino, J., Morin, S., Frey, M. M., Frosini, D., Vince, E., and Martins, J. M. F.: Air–snow transfer of nitrate on the East Antarctic Plateau – Part 1: Isotopic evidence

for a photolytically driven dynamic equilibrium in summer, *Atmos. Chem. Phys.*, 13, 6403–6419, doi:10.5194/acp-13-6403-2013, 2013.

Fisher, F. N., King, M. D., and Lee-Taylor, J.: Extinction of UV-visible radiation in wet mid-latitude (maritime) snow: Implications for increased NO_x emission, *J. Geophys. Res.*, 110, doi:10.1029/2005JD005963, 2005.

France, J. L., King, M. D., and Lee-Taylor, J.: The importance of considering depth-resolved photochemistry in snow: a radiative-transfer study of NO₂ and OH production in Ny-Alesund (Svalbard) snowpacks, *J. Glaciol.*, 56, 655–663, 2010.

France, J. L., King, M. D., Frey, M. M., Erbland, J., Picard, G., Preunkert, S., MacArthur, A., and Savarino, J.: Snow optical properties at Dome C (Concordia), Antarctica; implications for snow emissions and snow chemistry of reactive nitrogen, *Atmos. Chem. Phys.*, 11, 9787–9801, doi:10.5194/acp-11-9787-2011, 2011.

Frey, M. M., Stewart, R. W., McConnell, J. R., and Bales, R. C.: Atmospheric hydroperoxides in West Antarctica: links to stratospheric ozone and atmospheric oxidation capacity, *J. Geophys. Res.*, 110, D23301, doi:10.1029/2005JD006110, 2005.

Frey, M. M., Hutterli, M. A., Chen, G., Sjostedt, S. J., Burkhart, J. F., Friel, D. K., and Bales, R. C.: Contrasting atmospheric boundary layer chemistry of methylhydroperoxide (CH₃OOH) and hydrogen peroxide (H₂O₂) above polar snow, *Atmos. Chem. Phys.*, 9, 3261–3276, doi:10.5194/acp-9-3261-2009, 2009.

Frey, M. M., Savarino, J., Morin, S., Erbland, J., and Martins, J. M. F.: Photolysis imprint in the nitrate stable isotope signal in snow and atmosphere of East Antarctica and implications for reactive nitrogen cycling, *Atmos. Chem. Phys.*, 9, 8681–8696, doi:10.5194/acp-9-8681-2009, 2009b.

Frey, M. M., Brough, N., France, J. L., Anderson, P. S., Traulle, O., King, M. D., Jones, A. E., Wolff, E. W., and Savarino, J.: The diurnal variability of atmospheric nitrogen oxides (NO and NO₂) above the Antarctic Plateau driven by atmospheric stability and snow emissions, *Atmos. Chem. Phys.*, 13, 3045–3062, doi:10.5194/acp-13-3045-2013, 2013.

Gallée, ~~H.~~ ~~H.~~ and Gorodetskaya, I.: [Validation of a limited area model over Dome C, Antarctic Plateau, during winter, *Clim. Dynam.*, 34, 61–72, doi:10.1007/s00382-008-0499-y, Preunkert, S., Jourdain, B., Argentini, 2010.](#)

[Gallée, H., Preunkert, S., Argentini, S., Frey, M. M., Genthon, C., Legrand, M., Jourdain, B., Pietroni, I., and Casasanta, G. Casasanta, G., Barral, H., Vignon, E., Amory, C., and Legrand, M.: Characterization of the boundary layer at Dome C during OPAL\(East Antarctica\) during](#)

[the OPALE summer campaign](#), *Atmos. Chem. Phys. Discuss., in press, 2014*, [15, 6225–6236](#), doi:10.5194/acp-15-6225-2015, 2015.

Honrath, R. E., Peterson, M. C., Dziobak, M. P., Dibb, J., Arsenaull, M. A., and Green, S. A.: Release of NO_x from sunlight-irradiated midlatitude snow, *Geophys. Res. Lett.*, 27, 2237–2240, 2000a.

Honrath, R. E., Guo, S., Peterson, M. C., Dziobak, M. P., Dibb, J. E., and Arsenaull, M. A.: Photochemical production of gas phase NO_x from ice crystal NO₃⁻, *J. Geophys. Res.*, 105, 24183–24190, 2000b.

Honrath, R., Lu, Y., Peterson, M., Dibb, J., Arsenaull, M., Cullen, N., and Steffen, K.: Vertical fluxes of NO_x, HONO, and HNO₃ above the snowpack at Summit, Greenland, *Atmos. Environ.*, 36, 2629–2640, doi:10.1016/S1352-2310(02)00132-2, 2002.

Jacobson, M. Z.: *Fundamentals of Atmospheric Modeling*, Cambridge University Press, Cambridge, UK, 1999.

Jones, A. E. and Wolff, E. W.: An analysis of the oxidation potential of the South Pole boundary layer and the influence of stratospheric ozone depletion, *J. Geophys. Res.*, 108, doi:10.1029/2003JD003379, 2003.

Jones, A. E., Weller, R., Anderson, P. S., Jacobi, H. W., Wolff, E. W., Schrems, O., and Miller, H.: Measurements of NO_x emissions from the Antarctic snow pack, *Geophys. Res. Lett.*, 28, 1499–1502, 2001.

Kaimal, J. and Finnigan, J. J.: *Atmospheric Boundary Layer Flows*, Oxford University Press, Oxford, UK, 1994.

King, J. C., Argentini, S. A., and Anderson, P. S.: Contrasts between the summertime surface energy balance and boundary layer structure at Dome C and Halley stations, Antarctica, *J. Geophys. Res.*, 111, D02105, doi:10.1029/2005JD006130, 2006.

Kukui, A., Legrand, M., Preunkert, S., Frey, M. M., Loisel, R., Gil Roca, J., Jourdain, B., King, M. D., France, J. L., and Ancellet, G.: Measurements of OH and RO₂ radicals at Dome C, East Antarctica, *Atmos. Chem. Phys.*, 14, 12373–12392, doi:10.5194/acp-14-12373-2014, 2014.

Lee-Taylor, J. and Madronich, S.: Calculation of actinic fluxes with a coupled atmosphere-snow radiative transfer model, *J. Geophys. Res.*, 107, 4796, doi:10.1029/2002JD002084, 2002.

Legrand, M., Preunkert, S., Jourdain, B., Gallée, H., Goutail, F., Weller, R., and Savarino, J.: Year-round record of surface ozone at coastal (Dumont d'Urville) and inland (Concordia) sites in East Antarctica, *J. Geophys. Res.*, 114, D20306, doi:10.1029/2008JD011667, 2009.

Legrand, M., Preunkert, S., Frey, M., Bartels-Rausch, Th., Kukui, A., King, M. D., Savarino, J., Kerbrat, M., and Jourdain, B.: Large mixing ratios of atmospheric nitrous acid (HONO) at Concordia (East Antarctic Plateau) in summer: a strong source from surface snow?, *Atmos. Chem. Phys.*, 14, 9963–9976, doi:10.5194/acp-14-9963-2014, 2014.

5 Lenschow, D. H.: Micrometeorological techniques for measuring biosphere–atmosphere trace gas exchange, in: *Biogenic Trace Gases: Measuring Emissions from Soil and Water*, edited by: Matson, P. A. and Harriss, R. C., Blackwell Science, London, 126–163, 1995.

Mayer, B. and Kylling, A.: Technical note: The libRadtran software package for radiative transfer calculations – description and examples of use, *Atmos. Chem. Phys.*, 5, 1855–1877, doi:10.5194/acp-5-1855-2005, 2005.

10 Meusinger, C., Berhanu, T. A., Erbland, J., Savarino, J., and Johnson, M. S.: Laboratory study of nitrate photolysis in Antarctic snow. I. Observed quantum yield, domain of photolysis, and secondary chemistry, *J. Chem. Phys.*, 140, 244305, doi:10.1063/1.4882898, 2014.

Neff, W., Helmig, D., Grachev, A., and Davis, D.: A study of boundary layer behavior associated with high NO concentrations at the South Pole using a minisodar, tethered balloons and sonic anemometer, *Atmos. Environ.*, 42, 2762–2779, doi:10.1016/j.atmosenv.2007.01.033, 2008.

[Oncley, S. P., Buhr, M., Lenschow, D. H., Davis, D., and Semmer, S. R.: Observations of summertime NO fluxes and boundary-layer height at the South Pole during ISCAT 2000 using scalar similarity, *Atmos. Environ.*, 38\(32\), 5389–5398, doi:10.1016/j.atmosenv.2004.05.053, 2004.](#)

20 Peterson, M. C. and Honrath, R. E.: Observations of rapid photochemical destruction of ozone in snowpack interstitial air, *Geophys. Res. Lett.*, 28, 511–514, 2001.

Preunkert, S., Ancellet, G., Legrand, M., Kukui, A., Kerbrat, M., Sarda-Estève, R., Gros, V., and Jourdain, B.: Oxidant Production over Antarctic Land and its Export (OPALE) project: an overview of the 2010–2011 summer campaign, *J. Geophys. Res.*, 117, doi:10.1029/2011JD017145, 2012.

25 Ridley, B., Walega, J., Montzka, D., Grahek, F., Atlas, E., Flocke, F., Stroud, V., Deary, J., Gallant, A., Boudries, H., Bottenheim, J., Anlauf, K., Worthy, D., Sumner, A., Splawn, B., and Shepson, P.: Is the Arctic surface layer a source and sink of NO_x in winter/spring?, *J. Atmos. Chem.*, 36, 1–22, doi:10.1023/A:1006301029874, 2000.

30 Roscoe, H., Brough, N., Jones, A., Wittrock, F., Richter, A., Roozendael, M. V., and Hendrick, F.: Characterisation of vertical BrO distribution during events of enhanced tropospheric BrO in Antarctica, from combined remote and in-situ measurements, *J. Quant. Spectrosc. Rad. Trans.*, 138, 70–81, doi:10.1016/j.jqsrt.2014.01.026, 2014.

Salawitch, R. J., Canty, T., Kurosu, T., Chance, K., Liang, Q., da Silva, A., Pawson, S., Nielsen, J. E., Rodriguez, J. M., Bhartia, P. K., Liu, X., Huey, L. G., Liao, J., Stickel, R. E., Tanner, D. J., Dibb, J. E., Simpson, W. R., Donohoue, D., Weinheimer, A., Flocke, F., Knapp, D., Montzka, D., Neuman, J. A., Nowak, J. B., Ryerson, T. B., Oltmans, S., Blake, D. R., Atlas, E. L., Kin-
5 nison, D. E., Tilmes, S., Pan, L. L., Hendrick, F., Van Roozendael, M., Kreher, K., Johnston, P. V., Gao, R. S., Johnson, B., Bui, T. P., Chen, G., Pierce, R. B., Crawford, J. H., and Jacob, D. J.: A new interpretation of total column BrO during Arctic spring, *Geophys. Res. Lett.*, 37, doi:10.1029/2010GL043798, 2010.

Simpson, W. R., King, M. D., Beine, H. J., Honrath, R. E., and Zhou, X.: Radiation-transfer modeling
10 of snow-pack photochemical processes during ALERT 2000, *Atmos. Environ.*, 36, 2663–2670, 2002.

Slusher, D. L., Neff, W. D., Kim, S., Huey, L. G., Wang, Y., Zeng, T., Tanner, D. J., Blake, D. R., Beyersdorf, A., Lefer, B. L., Crawford, J. H., Eisele, F. L., Mauldin, R. L., Kosciuch, E., Buhr, M. P., Wallace, H. W., and Davis, D. D.: Atmospheric chemistry results from the ANTCI 2005 Antarctic
15 plateau airborne study, *J. Geophys. Res.*, 115, D07304, doi:10.1029/2009JD012605, 2010.

Stull, R. B.: An Introduction to Boundary Layer Meteorology, Kluwer Academic Publishers, Dord-
brecht/Boston/London, 1988.

Theys, N., Van Roozendael, M., Hendrick, F., Yang, X., De Smedt, I., Richter, A., Begoin, M., Errera, Q., Johnston, P. V., Kreher, K., and De Mazière, M.: Global observations of tropospheric
20 BrO columns using GOME-2 satellite data, *Atmos. Chem. Phys.*, 11, 1791–1811, doi:10.5194/acp-11-1791-2011, 2011.

[Van Dam, B., Helmig, D., Neff, W., and Kramer, L.: Evaluation of Boundary Layer Depth Estimates at Summit Station, Greenland, *J. Appl. Meteor. Climatol.*, 52, 2356–2362, doi:10.1175/JAMC-D-13-055.1, 2013.](#)

25 Van Dijk, A., Moen, A., and De Bruin, H.: The principles of surface flux physics: theory, practice and description of the ECPACK library, Internal Report 2004/1, Meteorology and Air Quality Group, Wageningen University, Wageningen, the Netherlands, 2006.

[Wang, Y. H., Choi, J., Zeng, T., Davis, D., Buhr, M., Huey, G., and Neff, W.: Assessing the photochemical impact of snow \$NO_x\$ emissions over Antarctica during ANTCI 2003, *Atmos. Environ.*, 41, 3944–3958, doi:10.1016/j.atmosenv.2007.01.056, 2007.](#)

30 [Wolff, E. W., Jones, A. E., Martin, T. J., and Grenfell, T. C.: Modelling photochemical \$NO_x\$ production and nitrate loss in the upper snowpack of Antarctica, *Geophys. Res. Lett.*, 29\(20\), doi:10.1029/2002GL015823, 2002.](#)

Zatko, M. C., Grenfell, T. C., Alexander, B., Doherty, S. J., Thomas, J. L., and Yang, X.: The influence of snow grain size and impurities on the vertical profiles of actinic flux and associated NO_x emissions on the Antarctic and Greenland ice sheets, *Atmos. Chem. Phys.*, 13, 3547–3567, doi:10.5194/acp-13-3547-2013, 2013.

Table 1. NO_x mixing ratios and flux at Dome C during 23 November 2011–12 January 2012.

Parameter	z, m	mean $\pm 1\sigma$	median	$t_{\text{total}}, \text{days}^a$
NO, pptv	–0.1 ^b	1097 \pm 795	879	2.9
	0.01	121 \pm 102	94	18.6
	1.0	98 \pm 80	77	24.4
	4.0	93 \pm 68	78	13.7
NO ₂ , pptv	–0.1 ^b	4145 \pm 2667	2990	2.6
	0.01	328 \pm 340	222	17.6
	1.0	211 \pm 247	137	23.2
	4.0	210 \pm 199	159	12.8
NO _x , pptv	–0.1 ^b	5144 \pm 3271	3837	2.6
	0.01	447 \pm 432	319	17.5
	1.0	306 \pm 316	213	23.2
	4.0	302 \pm 259	241	12.8
F–NO _x $\times 10^{13}$ molecule m ^{–2} s ^{–1c}	0.01–1.0	2.5 \pm 8.2	1.6	17.4
F–NO _x $\times 10^{13}$ molecule m ^{–2} s ^{–1} , local noon	0.01–1.0	5.0 \pm 8.2	2.9	1.1
F–NO _x $\times 10^{13}$ molecule m ^{–2} s ^{–1} , local midnight	0.01–1.0	0.3 \pm 1.6	0.4	0.2

^a Total sample time estimated as the sum of all 1 min intervals.

^b Firm air sampled during 20–22 December 2011, 1–5 January 2012 and 10–14 January 2012.

^c 1 December 2011–12 January 2012.

Table 2. Seasonal evolution of median NO_x mixing ratios and flux along with relevant environmental parameters at Dome C in summer 2011–2012 (time periods I.–IV. highlighted in Fig. 1 and 7) and comparison to summer 2009–2010 (from Frey et al., 2013).

Parameter	I. 23 Nov 2011– 30 Nov 2011	II. 1 Dec 2011– 8 Dec 2011	III. 9 Dec 2011– 22 Dec 2011	IV. 23 Dec 2011– 12 Jan 2012	9 Dec 2009– 22 Dec 2009	23 Dec 2009– 12 Jan 2010
NO_x (pptv) ^a	180	324	451	122	183	145
$\text{F-NO}_x \times 10^{13}$ (molecule $\text{m}^{-2} \text{s}^{-1}$) ^b	–	0.94	3.10	1.30	–	0.66
ΔNO_x (pptv) ^b	–	–63	–153	–51	–	–32
$\text{NO}_2 : \text{NO}$ ^a	1.3	1.5	2.8	2.0	1.1	0.60
T_{air} ($^{\circ}\text{C}$)	–34.5	–34.5	–31.0	–27.4	–31.5	–30.9
wind speed (m s^{-1})	6.3	3.0	2.5	3.8	2.4	2.2
K_h ($\text{m}^2 \text{s}^{-1}$)	–	0.046	0.049	0.080	–	0.043
h_z (m) ^c	–	19	20	36	6–59	18–25
$J_{\text{NO}_3^-} \times 10^{-8}$ (s^{-1})	–	–	2.93	2.68	–	–
SZA ($^{\circ}$)	69.7	68.1	67.6	67.9	67.6	67.9
column O_3 (DU)	301	294	272	297	311	309
NO_3^- skin layer (ng g^{-1}) ^d	513	764	1090	439	866	1212
O_3 (ppbv)	34.2	35.7	31.9	21.1	24.6	22.6

^a At 1 m above the snow surface.

^b Based on concentrations at 1.0 and 0.01 m above the snow surface.

^c Model estimates.

^d From daily sampling of the top 0.5 cm of snow.

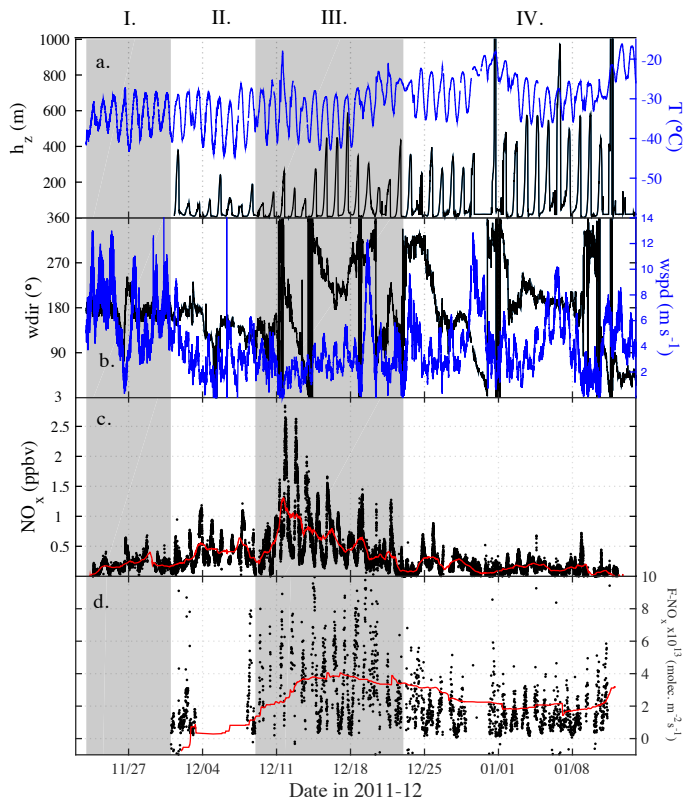


Figure 1. Meteorology and NO_x observations at Dome C in summer 2011–2012 (highlighted periods I.–IV. as referred to in text and Table 2): **(a)** air temperature (T) at 1.6 m and modeled mixing height (h_z) (Gallée et al., 2015), **(b)** wind speed (wspd) and direction (wdir) at 3.3 m **(c)**, 1 min averages of NO_x mixing ratios at 1 m (red line is 1 day running mean) and **(d)** 10 min averages of observational estimates of NO_x flux (F_{NO_x}) between 0.01 and 1 m (red line is 14 day running mean).

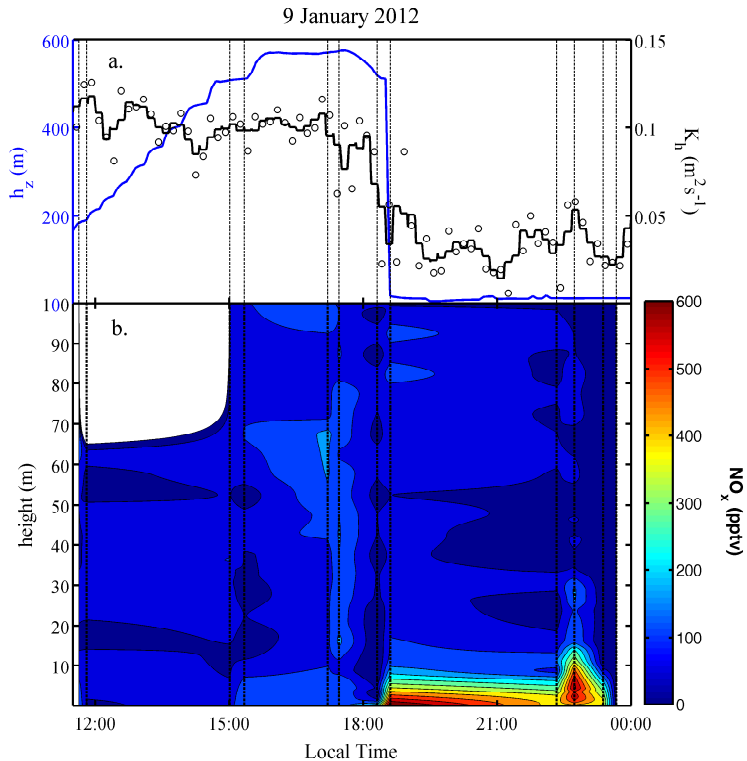


Figure 2. Balloon profiles (vertical dashed lines) from 9 January 2012: **(a)** modelled mixing height h_z (10 min running mean) and observed turbulent diffusion coefficient of heat K_h at 1 m (symbols: 10 min averages and black line: 30 min running mean) at 1. **(b)** interpolated vertical profiles of NO_x mixing ratios with contour lines representing 60 pptv intervals. The lower 100 m appear well mixed during the day, while after collapse of the convective boundary layer in the early evening NO_x emissions are trapped near the surface causing a strong increase in mixing ratios near the ground.

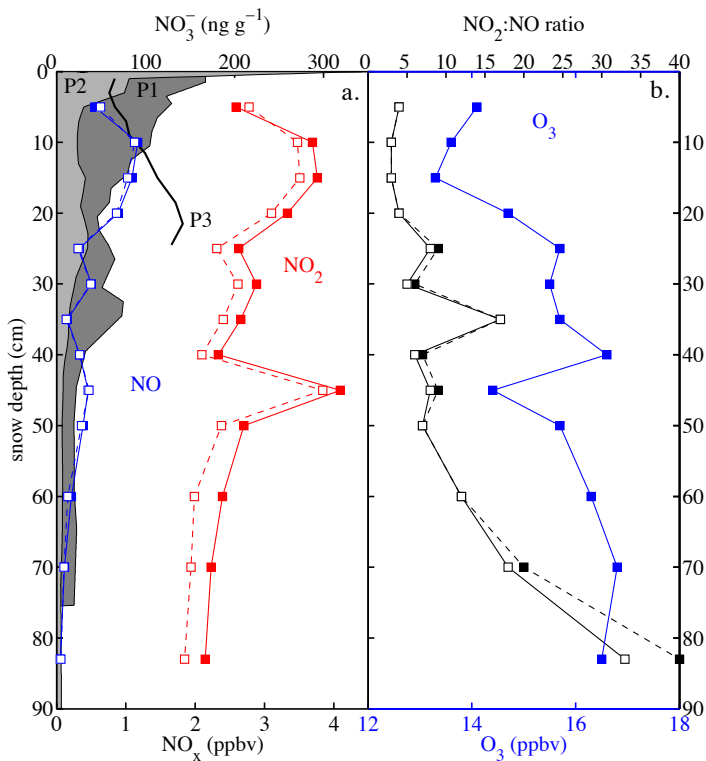


Figure 3. Firn air mixing ratios of (a) NO_x and (b) O₃ observed on 12 January 2012. Symbols represent 30 min averages. Solid and dashed lines are results from a 20 m and 50 m long intake lines, respectively. Shown are also NO₃⁻ concentrations in snow at 100 m (P1) and 5 km (P2) distance from the lab shelter as well as from under the firn probe (P3).

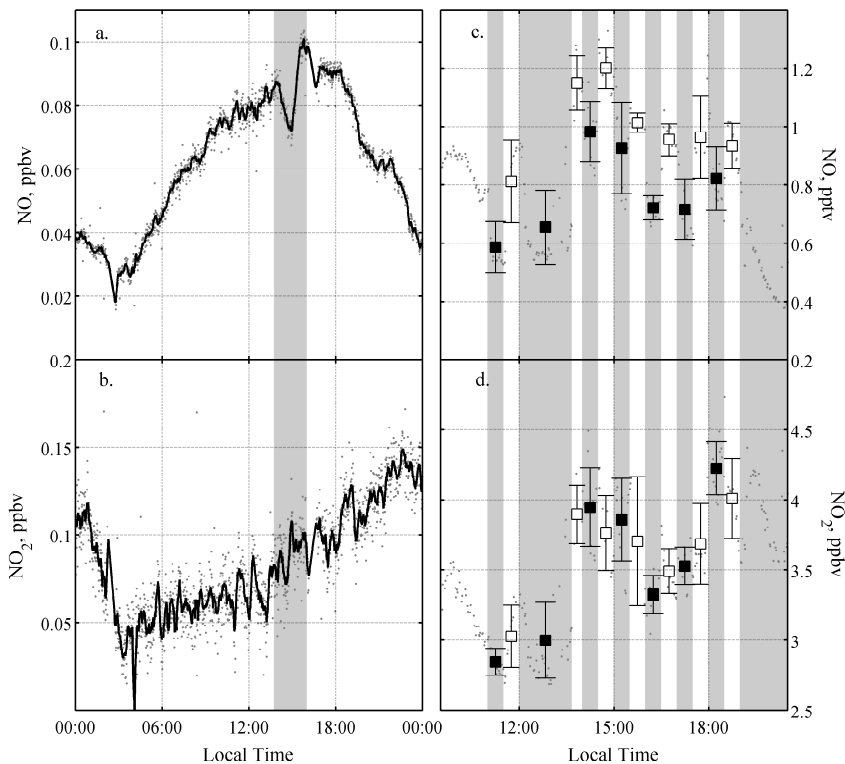


Figure 4. The impact of rapid changes in incident solar radiation on atmospheric NO_x mixing ratios (1 min values). **(a–b)** ambient concentrations at 1 m during a partial solar eclipse on 25 November 2011 (shaded area) with black lines representing the 10 min running mean. **(c–d)** firn air concentrations at 10 cm depth during a shading experiment using UV-filters on 11 January 2012. Square symbols and error bars represent interval averages and [SD standard deviation](#), respectively. Shaded areas and filled squares indicate time periods when the UV filter was in place.

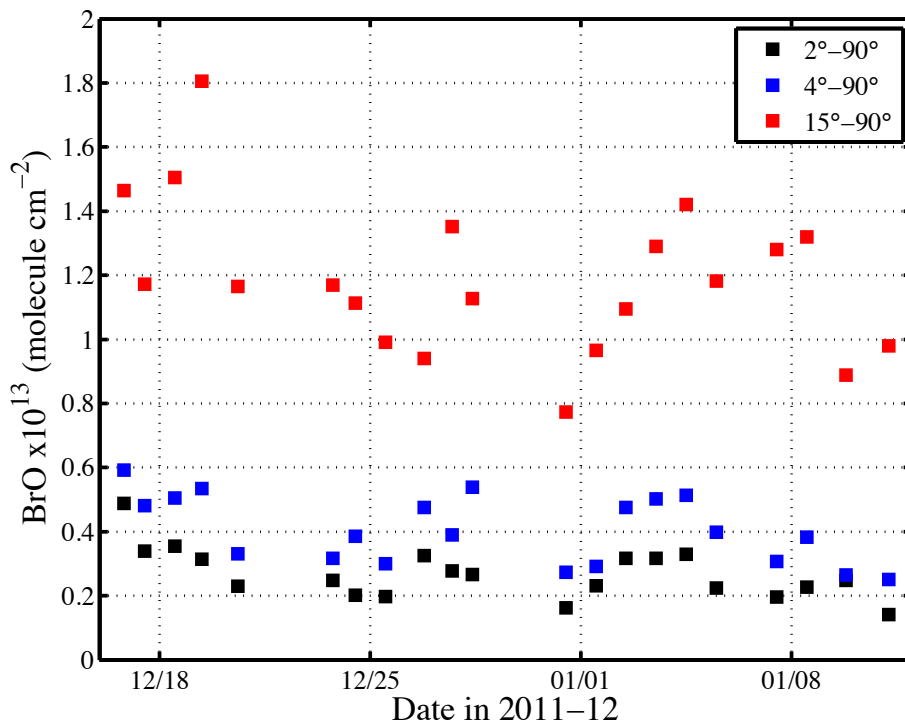


Figure 5. Median daily values of MAX-DOAS BrO vertical amounts from Dome C during sunny days or part-days only, after subtracting zenith amounts (see text). Reference spectrum from near-noon on 18 December until 6 January, then from near noon on 7 January. The apparently larger vertical amounts at higher elevations show that much of the BrO is in the free troposphere.

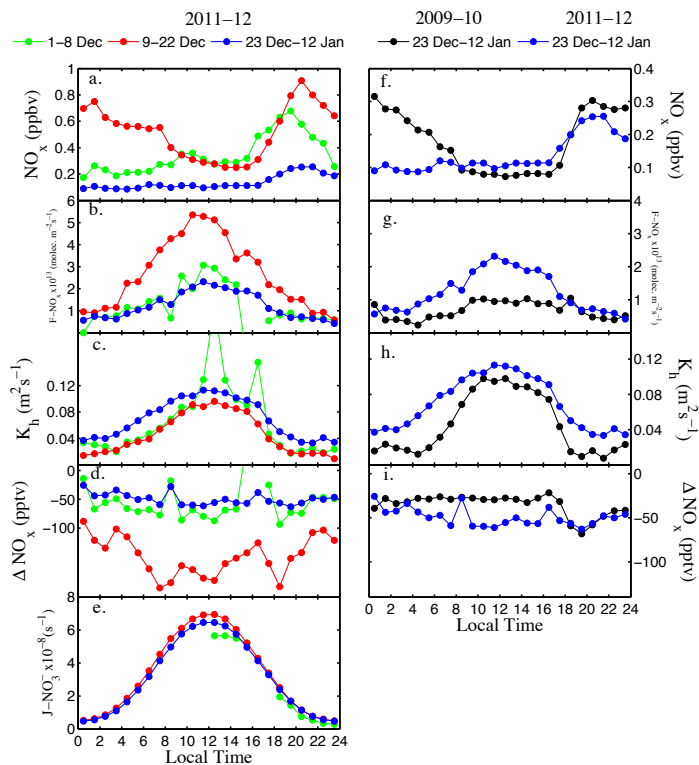


Figure 6. Observed median diurnal cycles during selected intervals in **2011–2012 (a–e)** **2011–2012** (referred to as periods II–IV in Table 2, Figs. 1, 7) and **2009–2010 (f–i)** **2009–2010**. Shown are **(a, f)** NO_x mixing ratios at 1 m **(a, f)**, **(b, g)** NO_x flux ($F\text{-NO}_x$) between 0.01 and 1 m **(b, g)**, **(c, h)** the turbulent diffusion coefficient of heat (K_h) at 1 m **(c, h)**, **(d, i)** the difference in NO_x mixing ratios (ΔNO_x) between 1.0 and 0.01 m **(d, i)**, and **(e)** the 2π downwelling nitrate photolysis rate coefficient ($J_{\text{NO}_3^-}$) **(e)**. Note comparable observations of $J_{\text{NO}_3^-}$ are not available from 2009–2010.

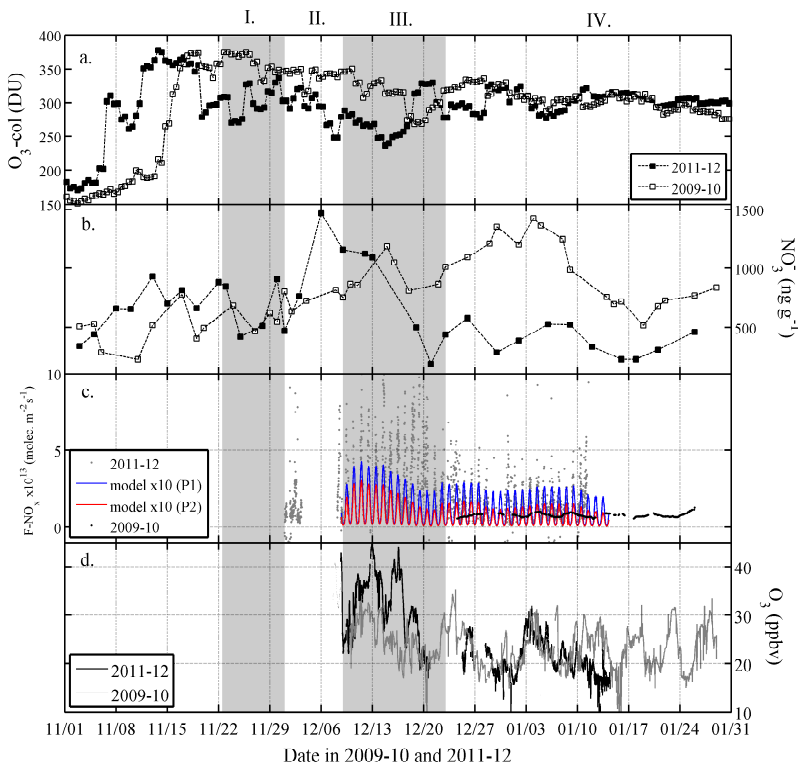


Figure 7. (a) Total column O_3 above Dome C. (b) NO_3^- concentrations in the skin layer of surface snow (top 0.5 cm). (c) observational estimates of NO_x flux (F_{NO_x}) between 0.01 and 1 m (10 min averages) and modelled F_{NO_2} (multiplied by 10) based on NO_3^- in the skin layer and depth profiles observed at 100 m (P1) and 5 km (P2) distance from the lab shelter (see Fig. 3a); the 1 day running mean of F_{NO_x} during 2009–2010 is shown for comparison (from Frey et al., 2013) (d) atmospheric O_3 mixing ratios. Highlighted periods I–IV, as referred to in text and Table 2.